NAZARBAYEV UNIVERSITY

NEXT-GENERATION SEQUENCING AND IMAGING FLOW CYTOMETRY ANALYSIS OF THE MICROBIAL COMMUNITIES OF ARAL SEA REMNANT LAKES

ALYAMDAR ASKEROV

(B.Sc. in Biological Sciences, Nazarbayev University)

A THESIS SUBMITTED IN PARTIAL FULFILLMENT OF THE REQUIREMENT OF NAZARBAYEV UNIVERSITY FOR THE DEGREE OF MASTER OF SCIENCE IN BIOLOGICAL SCIENCES AND TECHNOLOGIES

APRIL 2023

Student:	Alyamdar Askerov	13/04/2023
Supervisor:	Dr. Natalie Barteneva	13/04/2023
Co-Supervisor:	Dr. Christian Schönbach	13/04/2023

Examiners

The M.Sc. thesis of Alyamdar Askerov has been approved by the examiners.

Dr. Attila Szabo, PhD, Swedish University of Agricultural Sciences, CER Institute of Aquatic Ecology

Dr. Vadim Yapiyev, PhD, School of Mining, Nazarbayev University, Environmental Science

Abstract

Once one of the largest lakes by area, the Aral Sea's water level decreased drastically within the last 60 years due to climate change and anthropogenic activity. This resulted in the emergence of several distinct saline and hypersaline water reservoirs, such as the Small Aral Sea, the West Aral Sea, and Chernyshev Bay.

This study is focused on: 1) the characterization of the epilimnion phytoplankton and bacterioplankton communities of the Chernyshev Bay and northern parts of West Aral Sea, and 2) the correlation of phytoplankton and bacterioplankton biodiversity to the set of environmental variables (e.g., temperature, conductivity, salinity, pH, and nutrient concentration). To accomplish this, water samples were collected from the Chernyshev Bay and the West Aral Sea (expedition Aral-2022), which were further analyzed by full-length 16S rRNA next-generation sequencing (NGS) for bacterioplankton diversity, and imaging flow cytometry (IFC) for phytoplankton diversity. The obtained bacterioplankton diversity was further analyzed using alpha-diversity metrics via Shannon and Simpson indices and Non-metric MultiDimantional Scaling (NMDS tests). Lastly, the effect of environronmental parameters was analyzed using the Principal Component Analysis (PCA). According to the IFC results, Chernyshev Bay, but not the Western Aral Sea, was dominated in October 2022 by Dunaliella spp.(up to 98%), which confirms the final separation of Chernyshev Bay Lake. Several filamentous cyanobacteria, diatomic algae, and representatives of Aulacoseira, Aphanocapsa, and Pediastrum genera were detected in Chernyshev Bay's water samples. NGS-based taxonomical analysis of bacteriome showed that there is a diversity dissimilarity between Chernyshev Bay and West Aral Sea and strong similarity among littoral and limnetic points within the Chernyshev Bay. According to the PCA result, conductivity and ammonium concentration were the most important environmental parameters. The patterns described here represent the first observation of bacteriome and phytoplankton distribution in Chernyshev Bay and West Aral parts of the former Aral Sea.

The significance of this study is the contribution to our current knowledge of biodiversity in the Aral Sea, using a combined approach of NGS and IFC analysis. The obtained data can potentially enhance the limnological research of local and foreign hypersaline lakes across the globe.

Next-generation sequencing and imaging flow cytometry analysis of the microbial communities of Aral Sea remnant lakes.

Alyamdar Askerov

Table of Contents

Chapter 1 – Introduction

1.1 Literature Review
1.1.1 Aral Sea disaster

Until 1960, the basin of Aral Sea was the 4th largest lake by area after Caspian Sea in Eurasia, Lakes Superior in North America and Lake Victoria in Africa (Izhitskiy et al., 2014; Shi et al., 2014; Massakbayeva et al., 2019). After that the drying process started, and the level of Aral Sea fall drastically within the last 60 years (Micklin, 2007; Yapiyev et al., 2017a; Ayzel and Izhitskiy, 2018; Izhitskaya et al., 2019). Intensive studies were conducted to analyze the reason behind one of the major environmental catastrophes of the last century (Raskin et al., 1992; Zavialov et al., 2003; Izhitskiy et al., 2016). It is usually considered that the main reason behind this change is a dual impact of anthropogenic processes and climate change (Micklin, 1988; Raskin et al., 1992; Izhtskiy et al., 2014; Yapiyev et al., 2017a; Chaudhari et al., 2018; Karami 2018).

Several expeditions and satellite altimetry measurements were conducted to describe the effect of anthropogenic activity on the dynamics of water level of the Aral Sea (Micklin, 1988; Zavialov et al., 2003; Micklin, 2007; Singh et al., 2012). According to them, the process began due to difference in the water inflow from Amu Darya and Syr Darya rivers, which are two major water suppliers of the sea (Zavialov et al., 2003; Micklin, 2007; Yapiyev et al., 2017a). The process began with the decrease in the water inflow from the Amu Darya river, which in turn caused the split of the Aral Sea into northern (Small Aral) and southern (Large Aral) parts (Zavialov et al., 2003; Izhitskiy et al., 2014; Izhitskaya et al., 2019). The process of drying continued in both parts until the establishment in 2005 of the Kok-Aral dam in the Small Aral, which restored its levels by accumulating the water coming from Syr Darya river in the north, but still there was a channel connecting it with the Chernyshev Bay (Micklin, 2007; Plotnikov et al., 2016; Aladin et al., 2020; Massakbayeva et al., 2020). However, such measure was not possible in the Large Aral, and the drying process continued, which in turn split it into the West Large Aral Sea (shortly West Aral Sea) and the East Large Aral Sea (shortly East Aral Sea) (Micklin, 2007; Singh et al., 2012). Due to the differences in the amount of evaporation and precipitation between the eastern and western parts of Large Aral Sea, the East Aral Sea completely disappeared (Micklin, 1988; Singh et al., 2012). The next step was the partial segregation of Chernyshev Bay (which located in the north of West Aral Sea) from the main waters of West Aral Sea, which were connected by the seasonally reappearing narrow water channel (Figure 1) (Oberhänsli et al., 2007; Izhitskaya et al., 2019; Sapozhnikov and Kalinina, 2019). Lastly, during our expedition in 2022, we observed the full separation of the Chernyshev Bay from the main waters of West Aral Sea.
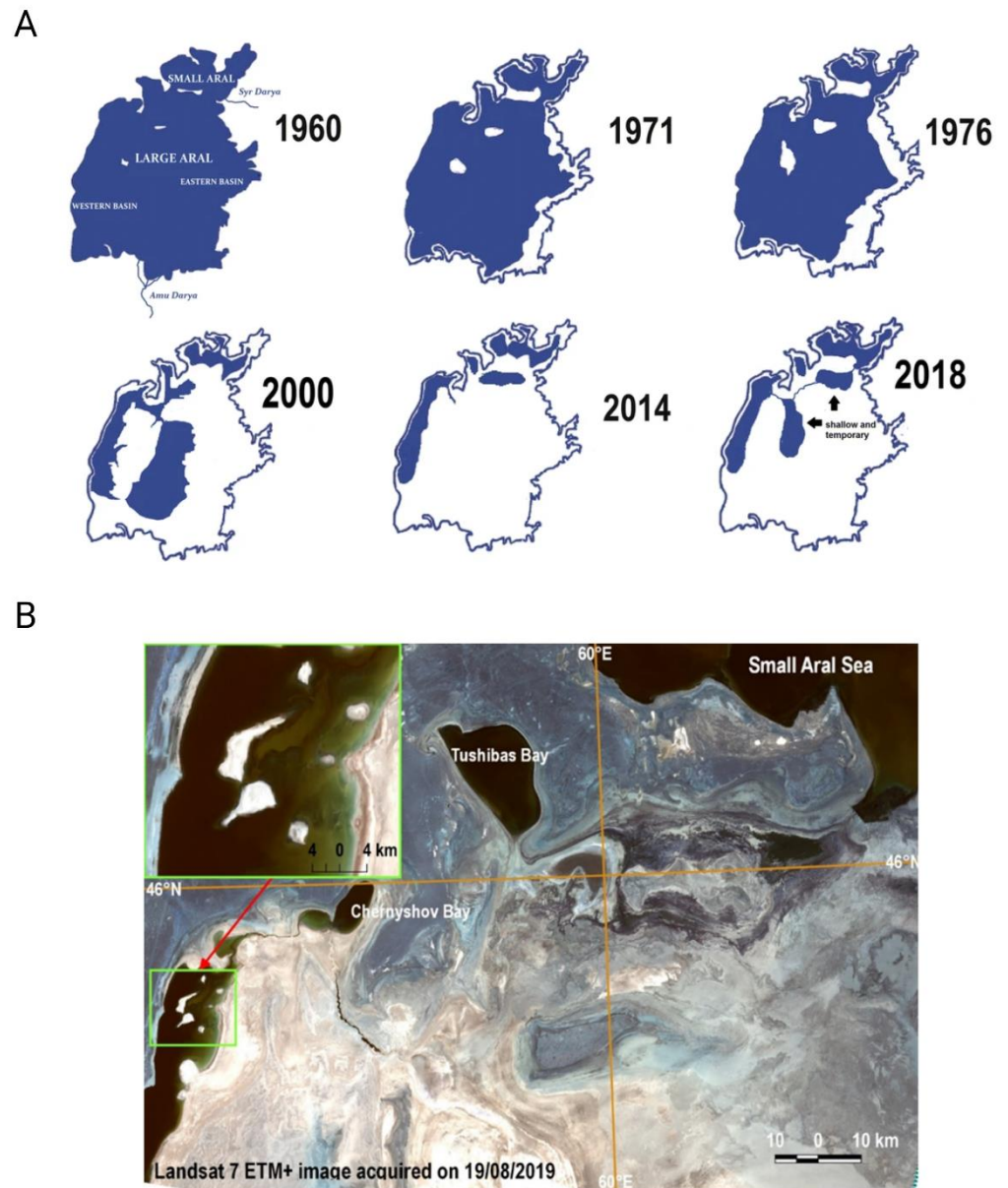
Figure 1. The change of Aral Sea profile: A) change over the last 6 decades (Aladin et al., 2018) B) the satellite image of Aral Sea territory taken on August 19, 2019, by Landsat 7 (the picture was used with the permission of Dr. Kanat Samarkhanov).

1.1.2 Aral Sea stratification

After the Aral Sea had segregated into several distinct water reservoirs, it was confirmed that each lake within the system had uneven precipitation and evaporation rates and this difference affects the temperature and salinity levels of the sea inducing the stratification process (Micklin, 1988; Small et al., 2001; Zavialov et al., 2003; Oberhänsli et al., 2007; Shurigin et al., 2019). The stratification process of the West Aral Sea was enhanced by the inflows of warmer and less salty waters from the East Aral (Zavialov et al., 2003; Boehrer and Schultze, 2008; Roget et al., 2009; Izhitskiy et al., 2014). From the data obtained in 2015, the stratified layers were present in the West Aral Sea and Chernyshev Bay (Izhitskaya et al., 2019). After the disappearance of the East Aral Sea, the western part still obtained seasonal stratification, which presumably was affected by the mix of groundwater due to the position

of the tectonic plates, which provides the supply of water that differs in its consistency (Jarsjö and Destouni, 2004; Oberhänsli et al., 2007; Boehrer and Schultze, 2008). In addition to the groundwater and external inflow, lake stratification may be originated from the process of photosynthesis of the microorganisms located at the epilimnion layer (uppermost layer) of the sea (Boehrer and Schultze, 2008). Lastly, the water interchange existed among the West Aral Sea, Chernyshev Bay, and Small Aral Sea through seasonal connections of water channels (Plotnikov et al., 2016; Aladin et al., 2020).

1.1.3 Aral Sea biodiversity

These dramatic changes created an endemic environment and impacted the biodiversity of the Aral Sea (Izhitskiy et al., 2016; Shurigin et al., 2019). The early studies were majorly focused on the change of the biodiversity of macroorganisms. However, according to Sapozhnikov and Kalinina (2019), the last large organisms inhabiting the Aral Sea were two fish species *(Atherina boyeri caspia, Platichthys flesus luscus)* and one bivalve mollusk species *(Syndosmya segmentum)*, which died out approximately in 2004 when the salinity levels reached 90ppt. It was stated in the works of Cretaux et al. (2005), that by reaching the levels of 300-350ppt, bacteria would become the only surviving organism. Starting from the last decade the levels of salinity in the Aral Sea reached extremely high, which allowed only hypersaline-tolerant microorganisms to survive (Izhitskiy et al., 2016; Sapozhnikov and Kalinina, 2019; Shurigin et al., 2019). At that point, the interest in the microbiome characterization of the Aral Sea had increased. The initial methods of investigation of water microorganisms involved light and electron microscopy. It was pointed out in the works of Sapozhnikov and Kalinina (2019) that the most diverse group of organisms inhabiting the Aral Sea are microorganisms, predominantly diatoms (*Navicula* spp, *Nitzschia* spp, *Halamphora* spp) and cyanobacteria (*Planktolyngbya* spp, *Synechocystis salina*). Only in recent years, there have been some trials in using molecular biology techniques, such as Next Generation Sequencing or gradient gel electrophoresis, to describe the biodiversity of the microbiome, providing the data of Archaea and saline-adapted Bacteria species (Izhitskiy et al., 2016; Shurigin et al., 2019; Begmanov et al., 2020; Alexyuk et al., 2021; Gao et al., 2021; Jiang et al., 2021). Unfortunately, majorly those studies were performed on the territory of Uzbekistan.

Prolonged exposure of lake surface to warm atmosphere favors the extensive growth of microbiome species and lake stratification (Sorokin et al., 2014; Yang et al., 2016). While the surface layers of thermally stratified lake may become warm and oxygen-rich, the bottom layers may stay cold and anoxic initiating biodegradation of organic matter, which in turn contributes to the methane accumulation (Izhitskaya et al., 2019). Additionally, the seasonal existence of channels, connecting West Aral Sea, Small Aral Sea and Chernyshev Bay, increases the stratification level and impacts the biodiversity of the corresponding region (Oberhänsli et al., 2007; Plotnikov et al., 2016; Izhitskaya et al., 2019; Aladin et al., 2020). The problems of surface blooms and bottom layer methane release enhances the lake stratification, and consequently impacts the climate change through the release of greenhouse gases (Raskin et al., 1992; Small et al., 2001; Boehrer and Schultze, 2008; Yapiyev et al., 2017b; Izhitskaya et al., 2019). That's why understanding the behavior of phytoplanktonic microbiome within the stratified lakes remains an important topic of research.

1.1.4 Phytoplankton investigation methods

There are several possible investigation methods of phytoplankton diversity analysis. The first method used for the analysis of the phytoplankton is light microscopy. This method primarily depends on the visual investigation of samples, where the classification is based on the morphological characteristics of organisms (Franks and Keafer, 2003; Guillard and Morton, 2003). This method is usually considered a standard method for phytoplankton characterization, but still, it highly depends on the level of the researcher's expertise. Also, if the species have high morphological similarity, it becomes even harder to differentiate them. An alternative method of optical analysis is imaging flow cytometry (IFC), which also provides the opportunity to differentiate the phytoplankton organisms according to their morphological features (Sellner et al., 2003; Dashkova et al., 2017; Mirasbekov et al., 2021). One of the IFC tools is the FlowCAM (Yokogawa Fluid Imaging Technologies, USA), the instrument that combines cytometry- and microscopy-based analysis (Dashkova et al., 2017; Stauffer et al., 2019). In addition to the visual images of the organisms, this tool allows one to precisely observe the sizes and diameters of cells within the fluid (Sellner et al., 2003; Stauffer et al., 2019).

1.1.5 Bacterioplankton investigation methods

As was mentioned above, in recent years the Next-Generation Sequencing (NGS) approach became a popular method of investigation, that provided us variety of tools (Gupta and Verma, 2019). There are several generations of the NGS that involve various technologies, such as pyrosequencing, reversible terminator sequencing, sequencing by ligation, Nanopore technologies , etc. (Szabo et al., 2017; Pichler et al., 2019; Gupta and Verma, 2019; Aszalos et al., 2020; Esenkulova et al., 2020) An examples of the sequencing platforms for the analysis of environmental samples are MiSeq by Illumina (USA) and MinION Oxford Nanopore (UK) (Yang et al., 2016; Winand et al., 2019; Aszalós et al., 2020 Esenkulova et al., 2020). Among these types of sequencing instruments preferences usually be given based on the aim of the research, since both of them have their advantages and disadvantages (Winand et al., 2019; Nygaard et al., 2020; Egeter et al., 2022). For example, sequencing platforms from Illumina (USA) have a lower rate of error during the sequencing, but they use shorter reads which decrease the sensitivity (Yang et al., 2016; Winand et al., 2019; Aszalós et al., 2020; Nygaard et al., 2020). On the other hand, Oxford Nanopore (UK)-based platforms use longer reads that allow researchers to identify the microbiome community diversity, however, it has a higher error percentage compared to Illumina (USA) (Nygaard et al., 2020; Mirasbekov et al., 2021; Egeter et al., 2022; Meirkhanova, 2022). Several studies suggested that the best option is to use them together in order to minimize the limitations of both methods (Winand et al., 2019; Egeter et al., 2022). Besides, the NGS approach can be used by itself for bacterioplankton analysis or it can be complimentary to the standard optical analysis such as light microscopy or IFC during phytoplankton analysis. (Yang et al., 2016; Mirasbekov et al., 2021; Meirkhanova, 2022).

1.2 Hypothesis

Considering the above-mentioned information this research was based on a complex approach, where the IFC analysis of phytoplankton was complemented by the Nanopore sequencing for characterization of the microbiome biodiversity up to the picoplankton level. It is hypothesized that the distribution of phytoplankton and bacterioplankton communities differ in the Chernyshev Bay from the West Aral Sea with the change in environmental variables of the two respective regions.

1.3 Aims

In order to test this hypothesis, a sequence of experiments was performed with a respect to the following aims:

Aim 1: To characterize the phytoplankton and bacterioplankton communities of West Aral Sea and Chernyshev Bay water samples by IFC and Oxford Nanopore-based NGS techniques respectively.

Aim 2: To analyze the relationships between microbiome diversity and environmental variables.

Chapter 2 – Materials and methods

2.1 Rationale

The method selection was based on the abovementioned aims. The water samples were collected in October 2022. As mentioned in aim 1 the main method of sequencing was Oxford Nanopore-based sequencing and the water samples in parallel were analyzed by imaging flow cytometry. Prior to the sequencing, a set of preparatory steps, such as DNA extraction and library construction was performed. The second aim is based on the establishing of relationship between quantitative data on phytoplankton and bacterioplankton diversities, and the differences in environmental variables such as pH, temperature, conductivity, phosphorous, and nitrogen concentrations. After finishing the data acquisition, the data analysis was conducted using the set of software such as Guppy, Kranken2, and Bracken. After this step was accomplished, the statistical analysis was performed, including α-diversity analysis, principal component analysis (PCA), and non-metric multidimensional scaling (NMDS) with a help of Graphpad (USA), and primer 7 (USA) software. A schematic overview of the experimental procedure is shown in Figure 2.
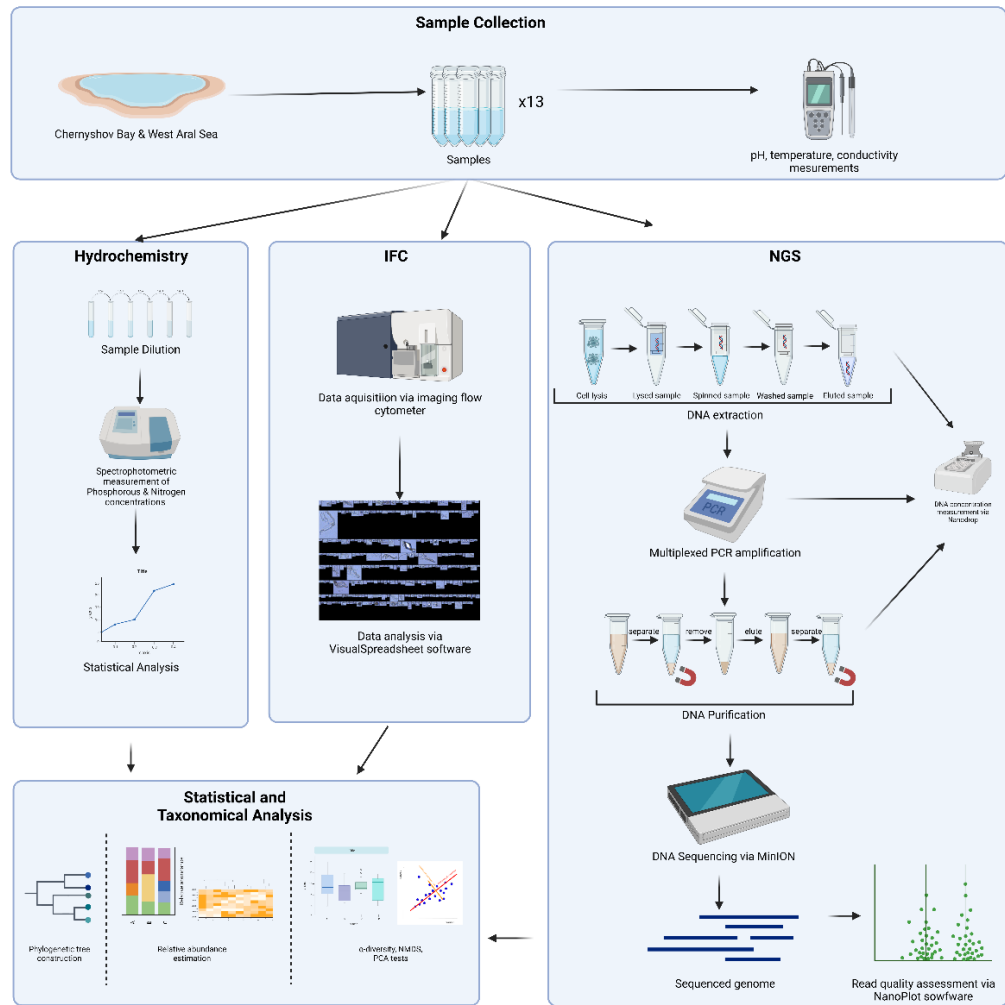
Figure 2. Schematic overview of the experimental process.

2.2 Experimental plan

2.2.1 Water sample collection

The process of sample collection was taken place during the expedition (Aral-2022) in the Chernyshev Bay and the West Aral Sea between October 3, 2022, and October 8, 2022. A total of 13 points were selected for the sample collection, where 11 of them were located in the Chernyshev Bay, and two were in the West Aral Sea. Then for each point, the temperature, pH, and conductivity were measured using a set of multimeters. The collected water was separated for further experiments, namely hydrochemistry, IFC, and Nanopore-based sequencing. The samples for IFC were fixed with 1% glutaraldehyde to preserve their natural state. The samples for sequencing were filtered immediately after collection, and the filters were stored in liquid nitrogen. The process was a collaborative effort of all members of Dr. Barteneva's lab.

2.2.2 Hydrochemistry analysis

2.2.2.1 Phosphorous content analysis

The total phosphorous concentration can be quantified by the conversion of inorganic phosphorous and organic-bound phosphorous into orthophosphate molecule (EPA, 1993). The principle consists of compound oxidation using potassium persulfate ($K_2S_2O_8$). The conversion process involves a series of different compound mixing dissolved in sulphuric acid solution. A sample with orthophosphate produces an antimony-12-phosphomolybdenum acid, when ammonium heptamolybdate (($NH_4)_6Mo_7O_{24}$) and potassium antimony (III) oxide tartrate ($K_2(SbO)_2C_8H_4O_{10}$) are added into the solution. Then the produced compound is mixed with the ascorbic acid which in turn produces the compound, called molybdenum blue, which amount is proportional to the orthophosphate content within the water sample. All 13 samples were analyzed according to this protocol, and the content of molybdenum blue was measured using spectrophotometer Evolution 300 (Thermo Fisher Scientific, USA) at 880nm. The absorbance values were compared to the calibration curve (attached in the Appendix 4), which was constructed according to the same protocol.

2.2.2.2 Nitrogen content analysis

The determination of the total inorganic nitrogen content was based on the measuring of concentration of the three most abundant ions within the sample, namely ammonium, nitrate, and nitrite ions. The measuring process was based on the Palintest protocol (YSI, USA):

Ammonium ion:

This method was based on the indophenol method, where ammonia reacted with alkaline salicylate, the resulting compound produces green-blue indophenol complex. This complex developed yellowish color and was proportional to the ammonia concentration. The absorbance of the complex was measured using the YSI 9500 Photometer (USA) at 650nm.

Nitrate ion:

This method was based on the reduction of nitrates to nitrites, and further determination by a diazonium reaction. This reaction of nitrites with sulfanilic acid forms reddish colored complex at the presence of N-(1-naphthyl)-ethylene diamine. The reddish complex's absorbance was measured using the YSI 9500 Photometer (USA) at 500nm and was proportional to the amount of nitrite ions. Zinc-based powder was used as a reaction catalyst. The standard protocol required the additional step of centrifugation for zinc-based powder removal from the solution. However, this concentration involved initial and reduced nitrite ions. To find the corrected concentration of nitrate ions it was required to find the concentration of initial nitrites.

<u>Nitrite ion:</u>

This method was similar to the nitrate concentration determination test, but it lacked the reduction stage, which means that only the initial nitrates present in the samples reacted with sulfanilic acid and formed reddish colored compound at the presence of N-(1-naphthyl)-ethylene diamine. The reddish complex concentration was measured using the YSI 9500 Photometer (USA) at 500nm and was proportional to the amount of nitrite ions initially present in the sample.

2.2.3 Imaging flow cytometry analysis

Priorly fixed samples were analyzed using the IFC technique. This procedure was done using FlowCAM VS-4 benchtop imaging flow cytometer (Yokogawa Fluid Imaging Technologies, USA). The FlowCAM instrument (Yokogawa Fluid Imaging Technologies, USA) was calibrated according to the manufacturer's protocol followed by the process of data acquisition from the liquid samples. Recommended magnification, which is suitable for phytoplankton analysis, was set up on the x10 objective in autoimage mode (Mirasbekov et al., 2021). This process was performed with a help of other lab members. The personal contribution involves the analysis of the obtained images using the VisualSpreadsheet software version 4 (Yokogawa Fluid Imaging Technologies, USA). Analysis of phytoplankton genera was conducted using the manual selection and semi-manual mode of software (Dashkova et al., 2017; Mirasbekov et al., 2021). The subsets of the genera were created based on statistical filtering where the threshold value would be established to the highest score value (Mirasbekov et al., 2021). The likeness value of an image was compared to the threshold value, where the images with the higher value were selected (Mirasbekov et al., 2021).

2.2.4 Next-generation sequencing

2.2.4.1 DNA extraction

The Whatman glass microfiber filters (Merck KGaA, Germany), pore size of 1.2 μm contained the material for sequencing and were stored in liquid nitrogen. Then after arriving back to the lab they were transferred to the -80°C fridge. After taking the samples from the fridge, the next stage was the DNA extraction. It was performed using the DNEasy Powerwater Kit (Qiagen, Germany). The standard manufacturer's DNA extraction protocol (Qiagen, Germany) was used for this purpose. According to the protocol, the samples were lysed by vortexing in the lysis buffer containing glass beads. The next step was the removal of proteins and inhibitors, followed by the DNA capturing in the spin column and the DNA elution. The concentration of eluted DNA will be further measured by Nanodrop (ThermoFisher Scientific, USA). Extracted DNA will be stored in the Eppendorf tubes (Germany) at -20°C.

2.2.4.2 Library construction

The process of library preparation for DNA sequencing started with PCR amplification. For this purpose, the 16S Barcoding Kit 1-24 (SQK-16S024) (Oxford Nanopore

Technologies, UK) was used for the barcoding of DNA samples. The procedure was conducted according to the manufacturer protocol, for which the set of following reagents is needed: 1) 5µL of nuclease-free water; 2) 25µL DreamTaq Hot Start PCR Master Mix; 3) 10µL of the corresponding 16S primer pair: (27F (5′-AGAGTTTGATCCTGGCTCAG-3′) and 1492R (5′-TACGGYTACCTTGTTACGACTT-3′)); 4) 10µL of DNA solution, where the DNA had 10ng by mass. The thermocycler was set up as follows: 1) Initial denaturation for 1 min at 95°C; 2) denaturation for 20 sec at 95°C (x 25 cycles); 3) Primer annealing for 30 sec at 55°C (x 25 cycles); 4) Extension for 2 min at 65°C (x 25 cycles); 5) Final extension for 5 min at 65°C. The obtained PCR products were cleaned using the AMPure XP beads (Beckman Coulter, USA), followed by the addition of sequencing adapters. In order to ensure the presence of DNA after abovementioned stages, the DNA concentration was measured after PCR amplification and PCR product purification using Nanodrop (ThermoFisher Scientific, USA).

2.2.4.3 Nanopore-based sequencing

After the library preparation step, the sample was sequenced using the MinION Mk1C device (Oxford Nanopore, UK). The process started with the priming of FLO-MIN106D flow cell (Oxford Nanopore, UK) using the flow cell priming kit EXP-FLP002 (Oxford Nanopore, UK). The next step was the mixing of the DNA library with loading beads, followed by the sequencing run which last about 40 to 46 hours.

2.2.4.4 Raw data analysis

Data analysis starts with data formatting followed by data analysis. Firstly, the sequencing data should be converted from raw data (FAST5 format) to analyzable data (FASTQ format) through the process of basecalling by Guppy neural network-based basecaller integrated into the MinION Mk1C device (Oxford Nanopore, UK). Further data manipulation involves several procedures:1) automatical demultiplexing and filtration (quality score of 7 and above) of the reads using Guppy (Oxford Nanopore, UK); 2) quality assessment using the NanoPlot package (https://github.com/wdecoster/NanoPlot); 3) classification of demultiplexed reads against SILVA database (v. 138.1) using Kraken2 (https://github.com/DerrickWood/kraken2), based on the exact k-mer matches to enhance the classification speed and accuracy up to genus level; 4) calculation of relative abundances using Bracken (https://github.com/jenniferlu717/Bracken); 5) taxonomical analysis using Pavian tool (https://github.com/fbreitwieser/pavian).

2.2.5 Statistical analysis

The statistical analysis involves the description of microbial communities based on the alpha diversity and beta diversity metrics using Vegan R package (https://github.com/vegandevs/vegan) and PRIMER-7 (PRIMER-e, New Zealand). It was used for α-diversity analysis, non-metric multidimensional scaling (NMDS) and principal component analysis (PCA).

2.2.6 Permits and approvals

This research did not require approval from NU IREC because it did not involve the work with human subjects or human material. The samplings were collected from the public area of northern parts of the West Aral Sea, that's why no additional permit required. Additionally, one of the members of the expedition was a representative of the Barsakelmes Nature Reserve, and field works were conducted with the representative's participation.

Chapter 3 – Results

3.1 Water sample collection

Overall, there was 13 water samples collected during the expedition conducted in October 2022. The samples were categorized according to the ecological zone and geographical location of collection. Table 1 provides the summary of the collected samples location and ecological zone category. According to it all points were assigned as follows: 7 points from the Chernyshev Bay's limnetic zone (CH_LIM_1 – CH_LIM_7), 4 points from the Chernyshev Bay's littoral zone (CH_LIT_1 – CH_LIT_4), and 2 points West from the West Aral Sea's littoral zone (WA1 – WA2).

Table 1. Summary of the collected samples' location. [*]

Point Name:	Ecological Zone:	Geographical Location:
CH_LIM_1	Limnetic	Chernyshev Bay
CH_LIM_2	Limnetic	Chernyshev Bay
CH_LIM_3	Limnetic	Chernyshev Bay
CH_LIM_4	Limnetic	Chernyshev Bay
CH_LIM_5	Limnetic	Chernyshev Bay
CH_LIM_6	Limnetic	Chernyshev Bay
CH_LIM_7	Limnetic	Chernyshev Bay
CH_LIT_1	Littoral	Chernyshev Bay
CH_LIT_2	Littoral	Chernyshev Bay
CH_LIT_3	Littoral	Chernyshev Bay

CH_LIT_4	Littoral	Chernyshev Bay	
WA1	Littoral	West Aral Sea	
WA2	Littoral	West Aral Sea	

* before the publication of a journal paper the geographical coordinates are available only upon request to PI of the project

3.2 Hydrochemistry analysis

The hydrochemistry analysis is the process of measuring the following water parameters: 1) pH; 2) temperature; 3) conductivity; 4) total phosphorous concentration; 5) nitrite concentration; 6) nitrate concentration; 7) ammonium concentration. Table 2 summarizes the above-mentioned water parameters across 13 points and the control group of ultrapure H_2O.

Table 2. Summarized hydrochemistry dataset.

	pH:	Temperature (ºC)	Conductivity (mS/cm):	Total phosphorous (mg/L):	Nitrite (mg/L):	Nitrate (mg/L):	Ammonium (mg/L):
CH_LIM_1	7.10	11.5	179.4	0.628	0.00	6.04	26.80
CH_LIM_2	7.26	14.4	189.0	0.626	0.00	0.00	20.00
CH_LIM_3	7.65	15.1	197.0	0.602	0.00	0.00	29.60
CH_LIM_4	7.55	14.5	191.0	0.584	0.02	0.80	36.80

CH_LIM_5	7.53	14.9	191.7	0.596	0.00	0.00	32.00
CH_LIM_6	7.55	15.1	192.7	0.502	0.00	0.00	34.40
CH_LIM_7	7.47	15.4	195.6	0.376	0.00	0.00	40.80
CH_LIT_1	7.20	13.0	106.5	0.580	0.00	0.00	31.60
CH_LIT_2	7.45	21.6	195.1	0.336	0.00	0.00	41.20
CH_LIT_3	7.41	21.6	190.3	0.658	0.00	0.00	33.60
CH_LIT_4	7.52	19.1	194.4	0.388	0.02	0.00	37.20
WA1	7.69	13.4	182.1	0.108	0.00	0.00	25.20
WA2	7.75	12.4	181.2	0.348	0.00	0.00	26.80

Temperature, pH, and conductivity were measured on the field, while the other measurements were conducted in the laboratory. The measurements of ion concentrations required an initial process of serial dilutions (initial measurements are attached to Appendix 3). Ultrapure H_2O was used as the negative control in each measurement conducted in the laboratory. The graphical visualization is represented in Figure 3.
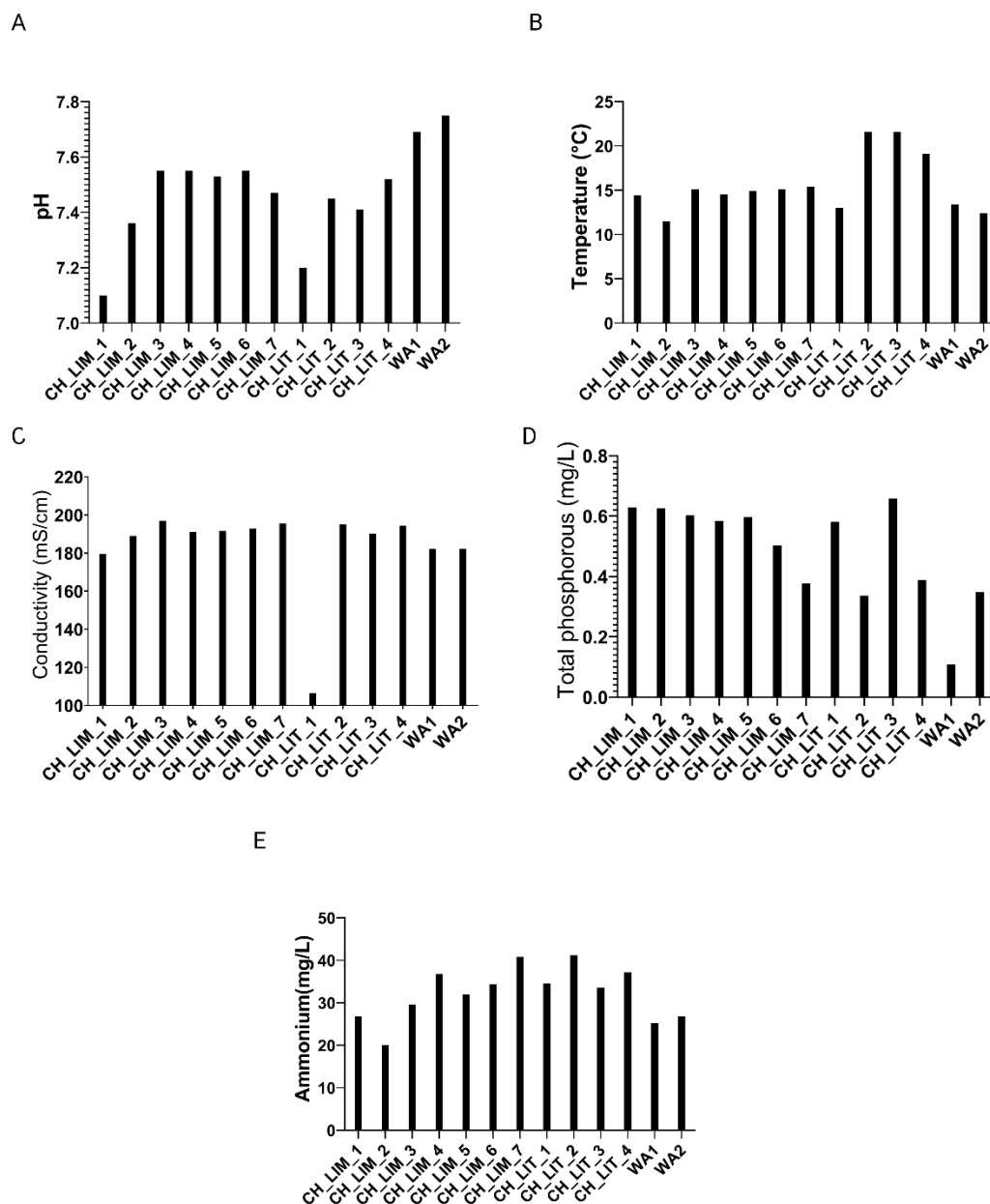
Figure 3. Summary of hydrochemistry measurements conducted in the Chernyshev Bay and the West Aral Sea. The x-axis (A-E) indicates the corresponding locations. The y-axis indicates a corresponding parameter as follows: A) pH; B) Temperature; C) Conductivity; D) Total phosphorous concentration; E) Ammonium ions concentration.

According to the pH measurements (Figure 3A), the values ranged from 7.10 up to 7.75 in the Chernyshev Bay, while in the West Aral Sea from 7.69 to 7.75. Overall, the values fell into the slightly alkaline zone. Since points WA1 and WA2 had the highest pH values, it may indicate that the West Aral Sea had higher alkalinity compared to the Chernyshev Bay. During comparison of ecological zones of Chernyshev Bay, the average values of pH were equal to 7.44 and 7.40 for the limnetic and littoral zones respectively, indicating almost identical acidity.

The temperature measurements (Figure 3B) differed across all points, and the tendency of temperature difference was dependent upon the time they were collected. Consequently, the comparison of geographical and ecological differences was not attainable.

With the exception of CH_LIM_1 and CH_LIT_1, the conductivity measurements (Figure 3C) of Chernyshev Bay indicated similar values across limnetic and littoral zones, and ranged from 189 mS/cm to 197 mS/cm. On the other hand, points from the West Aral Sea showed lower values of conductivity, 182.1 for WA1 and 181.2 for WA2, which may represent a slightly lower values of conductivity of West Aral Sea, compared to Chernyshev Bay

Next, the total phosphorous concentration measurements (Figure 3D) showed higher values in the Chernyshev bay (0.336 – 0.658 mg/L) than in the West Aral Sea (0.108 – 0.348 mg/L). Within the Chernyshev Bay the concentration of phosphorous was approximately equal at 5 limnetic zone points (CH_LIM_1 – CH_LIM_5), and on average were equal to 0.607 mg/L. The exceptions were points CH_LIM_6 and CH_LIM_7 where the corresponding concentrations were lower (0.502 mg/L and 0.376 mg/L respectively). However, in the littoral zone there was no tendency across the points (CH_LIT_1 – CH_LIT_4).

Since nitrite and nitrate were negligible or absent in majority of point, the graph (Figure 3E) only represented ammonium ions concentration. Overall, the graphical data did not exhibit a discernible pattern or trend, however, the values of ammonium concentrations in the West Aral Sea were slightly lower (25.20 – 25.80 mg/L) than in the Chernyshev Bay (20.00 – 41.20 mg/L). The average values of Chernyshev bay's limnetic and littoral zones' ammonium concentrations were equal to 31.4 mg/L and 35.9 mg/L respectively.

3.3 Phytoplankton analysis by IFC

Based on the IFC results, the Chernyshev Bay's water samples exhibited higher number of phytoplankton cells (4522 – 8467) compared to the West Aral Sea's samples (23 – 139). However, phytoplankton community in Chernyshev Bay was dominated by green algae, that belongs to *Dunaliella* genus (Figure 4) Its percentage abundance in the littoral zone of Chernyshev Bay was higher than 98% of all phytoplankton organisms (Figure 4B). On the other hand, IFC analysis of the West Aral Sea identified the negligible amount (2.1% in WA2) or the complete absence (0% in WA1) of *Dunaliella* spp. (Figure 4B). Since *Dunaliella* spp. cells contain high concentration of β-carotene (Figure 4C), the on-site picture indicates the potential blooming of the Chernyshev Bay with *Dunaliella* spp. (photo at Figure 4D).

Additionally, analysis of IFC images showed that *Aulacoseria* spp., aff. *Aphanocapsa salina*, filamentous cyanobacteria, diatomic algae, *Aulacoseria* spp, and *Pediastrum* spp. were also presented in low numbers within the waters of Chernyshev Bay (Figure 5). Potentially this indicates that the total phytoplankton diversity was higher in Chernyshev Bay than in the West Aral Sea.
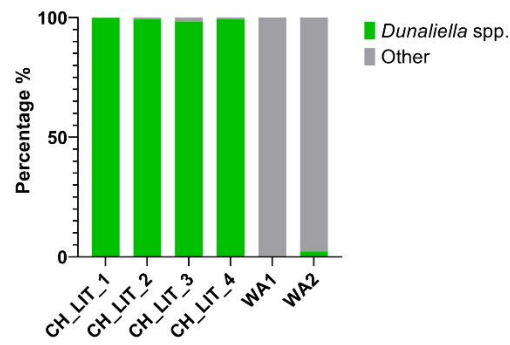
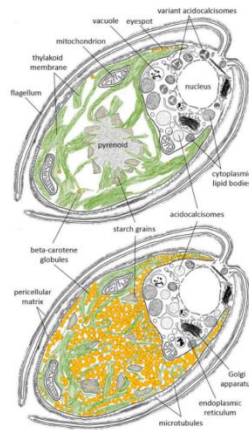**Figure 4.** *Dunaliella* spp analysis results of Chernyshev Bay and West Aral Sea: A) *Dunaliella* spp images obtained from CH_LIT_1; B) percentage abundance of *Dunaliella* spp across the Chernyshev Bay and the West Aral Sea; C) Schematic image of *Dunaliella salina* (Polle et al., 2020b); D) On site image of Chernyshev Bay representing the reddish water due to the presence of *Dunaliella* spp. (Aral-2022 expedition).
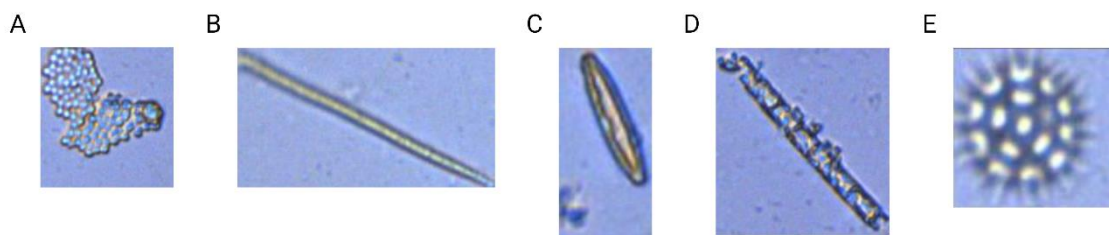
Figure 5. Images of Chernyshev Bay's non-dominant genera found in trace amounts: A) aff. *Aphanocapsa salina*; B) filamentous cyanobacteria; C) *Navicula* spp.; D) *Aulacoseira* spp.; E) *Pediastrum* spp.

3.4 Bacterioplankton analysis by NGS

3.4.1 Read quality assessment

After the sequencing was finished, the raw reads were undergone the base-calling process using guppy software with a minimum quality score of 7. Afterward, to confirm that the reads with lower quality were trimmed from the dataset a report containing the data before and after the filtering was constructed using NanoPlot software (Table 3).

Table 3. NanoPlot general summary before and after filtering by the quality score (>Q7).

	Before filtering:	**After filtering:**
Active channels:	479	467
Mean read length:	1525.7	1554.8
Mean read quality:	10.6	11.8
Median read length:	1581.0	1588.0
Median read quality:	11.0	11.8
Number of reads:	4509518	2369019
Read length N50:	1583.0	1589.0
STDEV read length:	457.0	215.7
Total bases:	6880251990	3683292292
Quality cutoff (>Q5):	4375208 (97.0%)	2369019 (100.0%)

Quality cutoff (>Q7):	3995212 (88.6%)	2369019 (100.0%)
Quality cutoff (>Q10):	2881925 (63.9%)	2016974 (85.1%)
Quality cutoff (>Q12):	1532586 (34.0%)	1070678 (45.2%)
Quality cutoff (>Q15):	36181 (0.8%)	24669 (1.0%)

According to the NanoPlot report all parameters had improved after the dataset of DNA reads was filtered based on the quality score. An increase in the mean and median length of reads as well as the increase in mean and median quality score after filtration is seen in the Table 3, which overall improved the further taxonomical and statistical analyses. Besides, the standard deviation of the read length was decreased after filtration, which indicates that there is less data dispersion compared to the mean length. The last 5 rows of Table 3 show the quality cutoff data across the DNA reads. It is seen that the number of reads in >Q5 and >Q7 became equal after the filtering process was done, which means that the trimming went successfully. To visualize the effect of filtering on the dataset, a graphical representation of read length vs average read quality is shown in the Figure 6. On the graph dots, x-axis, and y-axis represent a particular DNA reads, read length, and average read quality respectively. It is seen that there are no dots below the average read quality of 7 and below.

Figure 6. Read length vs Average read quality graphs constructed using NanoPlot: A) before the filtering by the quality score; B) after filtering by the quality score (>Q7).

3.4.2 Taxonomical analysis of bacterioplankton

The first stage of taxonomical analysis involved the process of read classification against the SILVA database using the Kraken2 software. The Kraken2 tool was based on the k-mer approach, which in turn involves the process of breaking the large DNA sequences into

subsequences of a certain length k (consequently being called k-mers). These k-mers were compared to the data of the SILVA database, which contains data about ribosomal RNA sequences of different lengths. Kraken2 generally uses a hierarchical approach where the compares the sequences with the database starting from the highest taxon and then narrowing down to the lowest taxon as more k-mers match references occur in the program. The lowest level of classification involved the genera-level taxon. The Kraken2 produced the corresponding kreport which was further used in the phylogenic tree production using the Pavian software (Appendix 4).

After the phylogenetic tree construction, the next stage of analysis involved the relative abundance estimation of genera across 13 points. The first step was the conversion of kreports to braken reports using the Braken software. The braken reports involved the data required to compute the total genera number and corresponding relative abundances in bacterioplankton DNA sequences.

The visual representation of total number of genera indicated within each location is represented on Figure 7. Overall, there is no certain trend in the number of genera. The lowest and highest number of identified genera was in location WA1 (83 genera), and WA2 (554 genera) respectively. With the exception of CH_LIM_6 (264 genera) and CH_LIM_7 (277 genera), the average number of genera within the Chernyshev Bay's limnetic points was approximately 403. Next, excepting the CH_LIT_1 (157) pint the average genera number within littoral zone of Chernyshev Bay was about 388.

The relative abundances of bacterioplankton genera were shown using heatmap (Figure 8). It involved the representation of the top 14 most abundant genera including some uncultured groups. The rest of the genera were summed into a separate group, called "Others". The visual analysis of the heatmap indicates high similarity in biodiversity and relative abundance of genera across all 11 points of Chernyshev Bay. In these points, the most abundant genera, which account for more than 75% of genera present within each location, are *Spiribacter* (19.96% - 30.36%), *Halopeptonella* (21.68% - 30.36%), *Halanaerobacter* (8.83% - 32.77%), and *Salinibacter* (5.56% - 12.66%). On the other hand, the West Aral Sea points showed a different data. Similarly, to the Chernyshev Bay, in WA1 there is a high abundance of genera such as *Spiribacter* (44.66%) and *Halopeptonella* (16.42%) accounting for about 61% of total abundance within the point, but *Halanaerobacter* and *Salinibacter* were in negligible amount (0.66% and 0.48% respectively). In WA2 the picture is slightly different, a high abundance corresponded to the *Spiribacter* (22.25%) and *Halopeptonella* (7.25%), *Halomonas* (34.94%) genera. However, *Halomonas* was in negligible amount in the Chernyshev Bay (less than 0.35%).
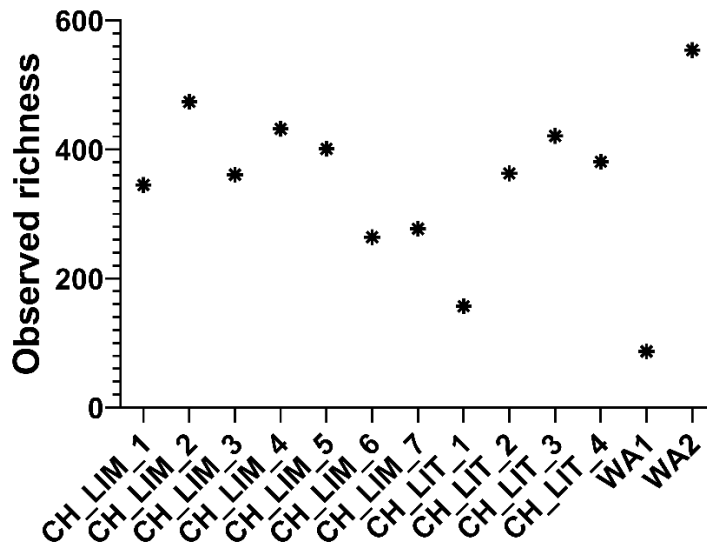
Figure 7. The graph shows the total bacterioplankton genera number across 13 locations in the Chernyshev Bay and the West Aral Sea

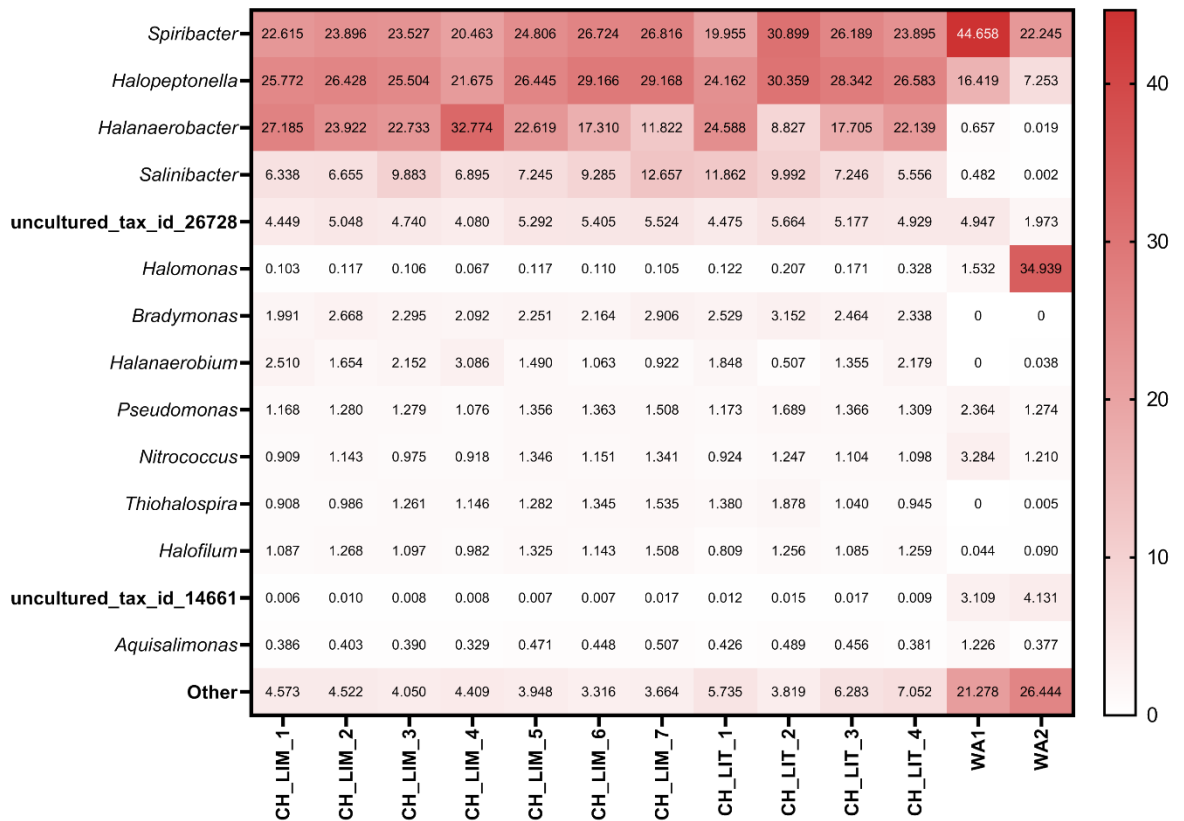|	CH_LIM_1	CH_LIM_2	CH_LIM_3	CH_LIM_4	CH_LIM_5	CH_LIM_6	CH_LIM_7	CH_LIT_1	CH_LIT_2	CH_LIT_3	CH_LIT_4	WA1	WA2
Spiribacter	22.615	23.896	23.527	20.463	24.806	26.724	26.816	19.955	30.899	26.189	23.895	44.658	22.245
Halopeptonella	25.772	26.428	25.504	21.675	26.445	29.166	29.168	24.162	30.359	28.342	26.583	16.419	7.253
Halanaerobacter	27.185	23.922	22.733	32.774	22.619	17.310	11.822	24.588	8.827	17.705	22.139	0.657	0.019
Salinibacter	6.338	6.655	9.883	6.895	7.245	9.285	12.657	11.862	9.992	7.246	5.556	0.482	0.002
uncultured_tax_id_26728	4.449	5.048	4.740	4.080	5.292	5.405	5.524	4.475	5.664	5.177	4.929	4.947	1.973
Halomonas	0.103	0.117	0.106	0.067	0.117	0.110	0.105	0.122	0.207	0.171	0.328	1.532	34.939
Bradymonas	1.991	2.668	2.295	2.092	2.251	2.164	2.906	2.529	3.152	2.464	2.338	0	0
Halanaerobium	2.510	1.654	2.152	3.086	1.490	1.063	0.922	1.848	0.507	1.355	2.179	0	0.038
Pseudomonas	1.168	1.280	1.279	1.076	1.356	1.363	1.508	1.173	1.689	1.366	1.309	2.364	1.274
Nitrococcus	0.909	1.143	0.975	0.918	1.346	1.151	1.341	0.924	1.247	1.104	1.098	3.284	1.210
Thiohalospira	0.908	0.986	1.261	1.146	1.282	1.345	1.535	1.380	1.878	1.040	0.945	0	0.005
Halofilum	1.087	1.268	1.097	0.982	1.325	1.143	1.508	0.809	1.256	1.085	1.259	0.044	0.090
uncultured_tax_id_14661	0.006	0.010	0.008	0.008	0.007	0.007	0.017	0.012	0.015	0.017	0.009	3.109	4.131
Aquisalimonas	0.386	0.403	0.390	0.329	0.471	0.448	0.507	0.426	0.489	0.456	0.381	1.226	0.377
Other	4.573	4.522	4.050	4.409	3.948	3.316	3.664	5.735	3.819	6.283	7.052	21.278	26.444

Figure 8. Heatmap showing the relative abundance of top 15 most abundant bacterioplankton genera across 13 locations in the Chernyshev Bay and West Aral Sea.

Due to the high presence of crustacean *Artemia* spp. within the basin of Chernyshev Bay, the abundance of chitin-degrading bacteria such as *Saccharospirillum* spp., *Arhodomonas* spp., and *Orenia* spp. was investigated as well (Figure 9). Overall, their

abundance across 13 locations was negligible, 0.008% - 0.088% for *Saccharospirillum* spp., 0.091% - 0.613% for *Arhodomonas* spp., and 0.064% - 0.210% for *Orenia* spp. Comparative analysis showed that *Saccharospirillum* spp. were indicated to be present in the Chernyshev Bay (0.008% - 0.027%) and the West Aral Sea (0.010% - 0.088%). *Arhodomonas* spp. were present in all points, but higher abundance was indicated in the West Aral Sea (0.231% - 0.613%) compared to the Chernyshev Bay (0.091% - 0.166%). Lastly, *Orenia* spp. were present only in the waters of Chernyshev Bay with almost identical abundance values for limnetic and littoral zones (0.103% - 0.210% and 0.064% - 0.204% respectively).
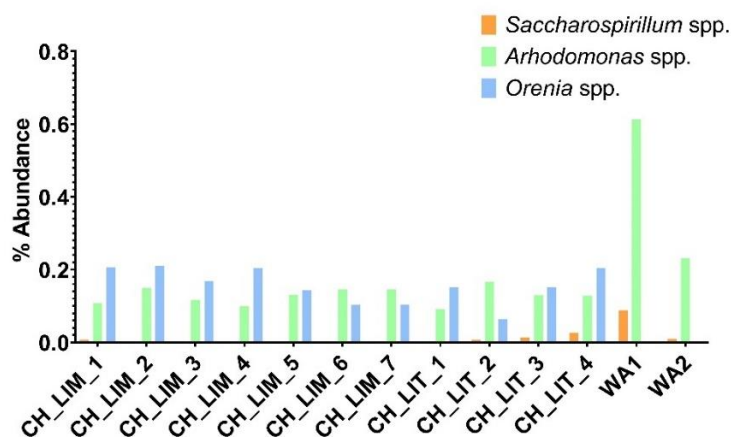
Figure 9. The graph of percentage abundance of chitin-degrading bacteria genera in the Chernyshev Bay and West Aral Sea.

3.5 Statistical analysis

3.5.1 α-Diversity analysis of bacterioplankton diversity

To estimate the bacterioplankton diversity of genera within each location an α-diversity test was conducted using the variations in Simpson and Shannon indices (Figure 10).

According to the Shannon index there is higher diversity within the West Aral Sea, where values were 2.37 for WA1 and 2.60 for WA2, in comparison, Chernyshev Bay had lower values ranged from 2.02 to 2.25. Evaluating Chernychev Bay's limnetic and littoral zones particularly, the limnetic location showed lower average value (2.07) than the littoral ones (2.16).

For the Simpson analysis, excluding the WA1 point where the index was equal to 0.76, the rest of the points showed approximately identical index values for the Chernyshev Bay and the West Aral Sea, which ranged from 0.79 to 0.82. Comparing limnetic and littoral zones of the Chernyshev Bay, the first ones were more identical to each other (0.80 – 0.81), while the second showed a higher range (0.79 – 0.82).

Potential reason that two indices showed different results lies in their derivation. The Shannon index usually makes emphasis on common as well as rare genera. This indicates that the West Aral Sea's rare genera increased the Shannon index-based bacterioplankton diversity

within the points. On the other hand, the Simpson index's emphasis usually comes from common only, and because the major genera involve only 5 groups (*Spiribacter, Halopeptonella, Halanaerobacter, Salinibacter,* and *Halomonas*) the index values were almost identical.

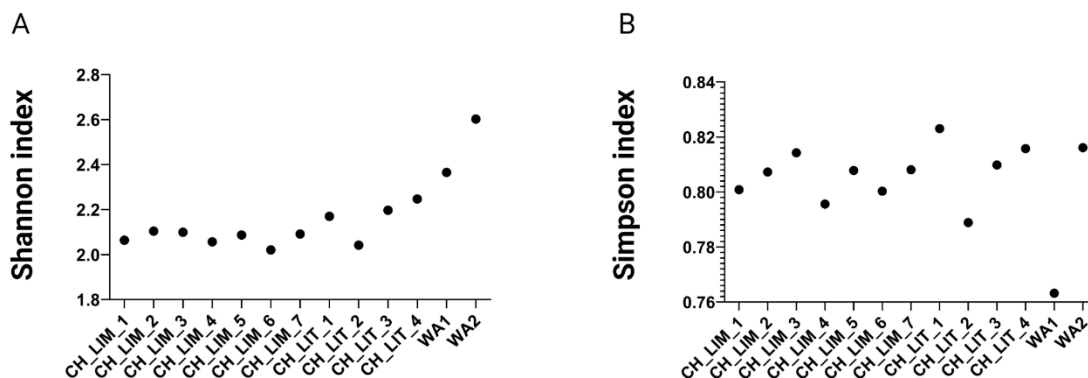**Figure 10.** Bar plots of α-diversity analysis of the Chernyshev Bay and the West Aral Sea: A) Shannon index; B) Simpson index.

3.5.2 NMDS analysis of bacterioplankton diversity

To visualize the dissimilarity across all 13 points, non-metric multidimensional scaling (NMDS) was conducted using the PRIMER-7 software (Figure 11). All points were color coded according to their geographical location, blue for the Chernyshev Bay and red for the West Aral Sea. As it seen from the NMDS, WA1 and WA2 points were segregated from the rest of dataset, which indicates that there is high dissimilarity in diversity between the West Aral Sea and Chernyshev Bay. All points from the Chernyshev Bay were located close to each other indicating their high similarity to each other. Both WA1 and WA2 are located separately from each other indicating a dissimilarity among the points of West Aral Sea. This data was also supported during the taxonomical analysis in Figure 8 and Figure 9.
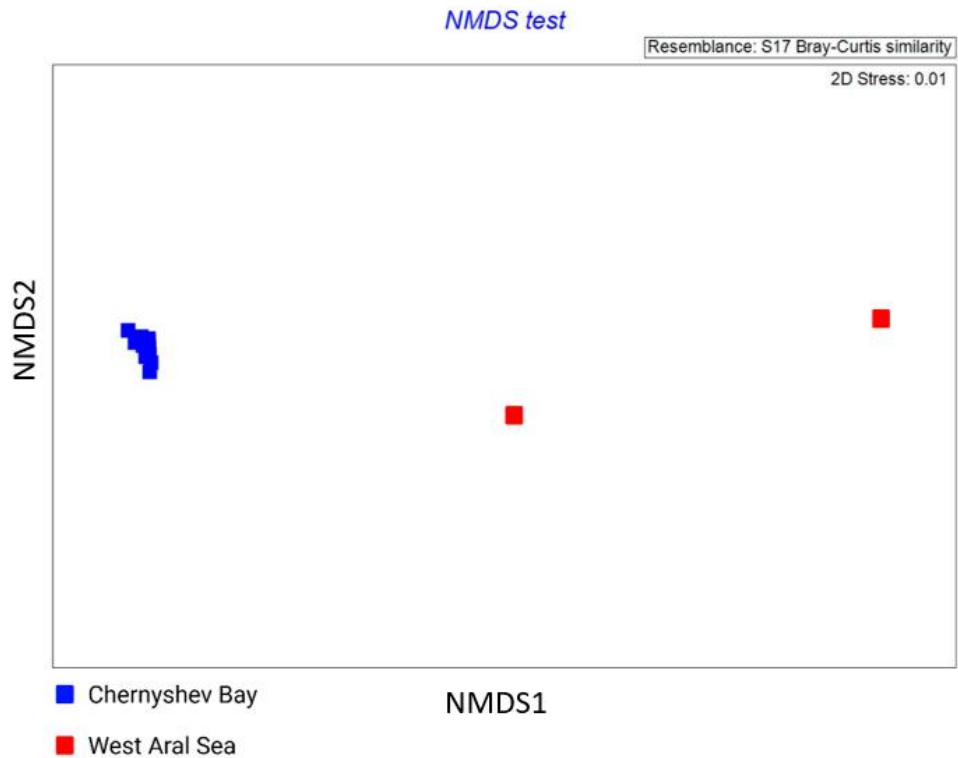
Figure 11. Non-metric multidimensional scaling (NMDS) ordination of Chernyshev Bay (blue) and West Aral Sea's (red) sample points based on the Bray-Curtis dissimilarity indices. Sample points are represented by colored dot that correlate with corresponding sample point.

3.5.3 PCA analysis of the environmental parameters

To estimate the impact of environmental variables on biodiversity, a principal component analysis (PCA) was using the data from Table 2 and illustrated on the Figure 12. X-axis of the graph corresponds to the Principal Component 1 (PC1), while y-axis to the Principal Component 2 (PC2). The proportion of variance for PC1 and PC2 was 92.36% and 6.88% respectively. Each vector corresponds to a particular environmental variable contribution to the dissimilarity, that may correlate with the diversity. Based on the magnitude of the vectors the top 2 most contributing variables to biodiversity of the Chernyshev Bay and the West Aral Sea were conductivity and ammonium concentrations, where the first one was highly correlated with the PC1 (Conductivity vs PC1 correlation = 1.000), and the second one highly correlated with the PC2 (Ammonium vs PC2 correlation = 0.974).
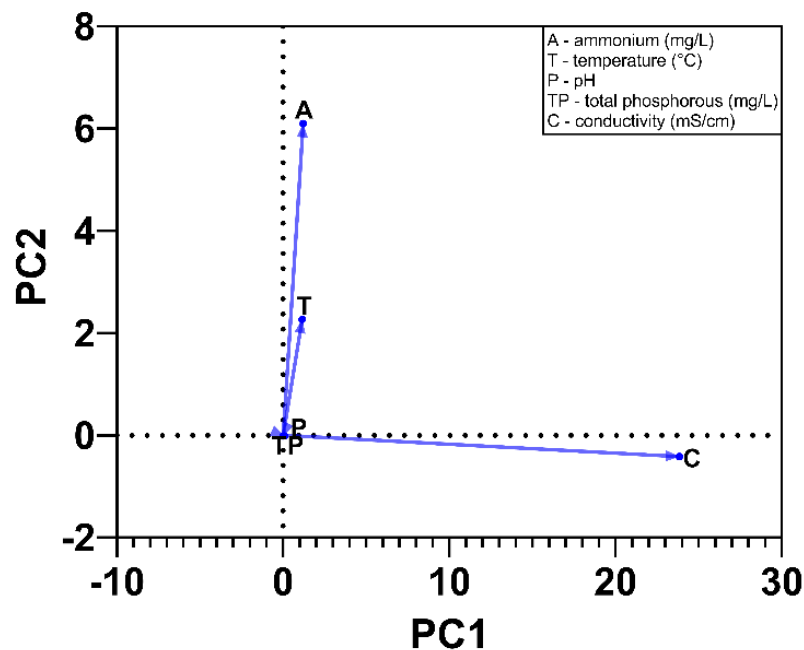
Figure 12. Principal Component Analysis (PCA) of ecological data in Chernyshev Bay and West Aral Sea. Parameters involved: pH, temperature, conductivity, phosphorous concentration, and ammonium ion concentration.

Chapter 4 – Discussion

Intensive research was conducted on the topic of aquatic phytoplankton and bacterioplankton communities' biodiversity analysis for their effect on the corresponding ecosystem. In particular, the studies of aquatic communities experiencing environmental problems are important for the impact of phytoplankton and bacterioplankton on climate change, nutrient cycles, and human health, and these are a few among many various fields of interest (Arrigo, 2005; Madsen, 2011; Zeglin, 2015; Verde et al., 2016; Salazar and Sunagawa, 2017; Chen et al., 2019).This study was focused on the characterization of phytoplankton and bacterioplankton communities using the complex approach consisting of IFC and Nanopore-based NGS taxonomical analyses within the basins of the Chernyshev Bay and the West Aral Sea, and their further correlation with environmental variables measured using common hydrochemistry methods.

4.1. Analysis of hydrochemistry trends of the Chernyshev Bay and West Aral Sea

The increase in salinity in the parts of the former Aral Sea was extensively described in the works of Zavialov et al. (2003), Mirabdullayev et al. (2004), Micklin (2016), and others. The general trend states that the salinization of the Aral Sea increases with the decrease of the water basin. In this study, we included the measurement of salt concentration conducted based on the conductivity measurements. Even though there were several trials on the conversion of conductivity to salinity and the traditional conversion methods are not applicable to the Aral Sea because of hypersalinity (Friedrich and Oberhänsli, 2004, Zavialov, 2010; Stunzhas, 2016). The empirical comparison of the conductivity values of this research to the data obtained in 2002 shows a 10-fold increase in conductivity in Chernyshev Bay (Friedrich and

Oberhänsli, 2004). The latest measurements of conductivity in the territory of the currently separated West Aral Sea were conducted in 2008, however, the measurements were adjusted with the use of a specific coefficient which may no longer be applicable due to the constant salt precipitation (Zavialov, 2010). Previously the trend of conductivity increase was usually explained in the context of salinity, where it states that salinity increase within the Aral Sea was the various effects of global warming and anthropogenic factors, which still may be applicable (Micklin, 1988; Raskin et al., 1992; Izhtskiy et al., 2014; Yapiyev et al., 2017a; Chaudhari et al., 2018; Karami 2018). The empirical explanation of conductivity trends requires additional data.

The pH values of the Aral Sea in 1947 reached values up to 8.0 (Friedrich and Oberhänsli, 2004). Then after the segregation of basins became significant in 2002, the pH measurements were taken separately for Chernyshev Bay and were slightly over 8.2 (Friedrich and Oberhänsli, 2004). By the year 2013, the pH value had changed to 8.11 (Makkaveev et al., 2016). The current study showed that pH values decreased and ranged from 7.10 to 7.69, which potentially indicates the tendency of Chernyshev Bay to become more acidic as it further splits from the West Aral Sea over the years. Temperature increase and consequent global warming may be the reasons behind the trend of acidification in Asian water reservoirs (Jamshidi and Bin Abu Bakar, 2011; Dutta et al., 2021). Also, the studies of other saline lakes showed that the pH values might show seasonal fluctuations (Jamshidi and Bin Abu Bakar, 2011). However, additional studies are needed to test it.

According to Friedrich and Oberhänsli (2004) in the summer of 2002, the phosphorous concentration was equal to 0.001-0.002 mg/L in Chernyshev Bay and about the same in the West Aral Sea. However, the increase in phosphorous concentration range was observed later in the West Aral Sea and was equal to 0.0014 – 0.0171 mg/L by 2012 (Makkaveev et al., 2016). Similar to the studies of Makkaveev et al. (2016), this work involves the analysis of total phosphorous concentration in littoral and limnetic zones. As stated previously, there was approximately similar phosphorous concentration across limnetic zone points, which ranged from 0.376 mg/L to 0.628 mg/L. On the other hand, there was no trend across the littoral zone, but concentration rage was equal to 0.108 mg/L – 0.658 mg/L. Overall is seen as a tendency to increase in total phosphorous concentration; however, it remains questionable why there such a significant change between 2016 and 2022 (Makkaveev et al., 2016).

According to the hydrochemistry analysis, the ammonium ion concentration had increased. Presumably, the increased ammonium concentrations follow the *Artemia* spp. concentration which was abundant in the West Aral Sea since the 1990s (Berdimbetova et al., 2019; Marden et al., 2020; Utemuratova et al., 2022). It is stated in the work of Marden et al. (2020) that the high concentration of ammonium ions in the Great Salt Lake results from the accumulation of excreted ammonium from *Artemia* spp., where its values reached over 50 mg/L in summer and slowly decreased in autumn. The measured values were still high, which may be explained as potential instrumental errors. However, this method was commonly used to assess freshwater samples and hypersaline ones (Reed et al., 2012; Berard et al., 2013; Makaya and Zuvarinopisa, 2019; Buzgeia et al., 2022). The concentration can be measured by alternative methodologies of total nitrogen concentration measurement (e.g., Kjeldahl digestion, persulphate oxidation) (Raveh and Avnimelech, 1979; Andrei et al., 2015).

4.2 IFC-based phytoplankton taxonomy analysis

Overall, the IFC analysis showed that phytoplankton diversity was higher in Chernyshev Bay compared to the West Aral Sea. Firstly, the most dominant phytoplankton organism was the halophilic algae *Dunaliella* spp. The presence of *Dunaliella* spp. was described in the previous studies of the Aral Sea and other hypersaline lakes as well (Oren, 2014; Barteneva et al., 2019; Mavzhudova et al., 2020; Mirzahasanlou and Hejazi, 2022). However, this work analysis showed that *Dunaliella* accounted for more than 98% of phytoplankton (> 2 μm size range) in the waters of Chernyshev Bay. The negligible amount and complete absence were observed in points WA2 and WA1, respectively. One of the reasons for its high amounts in Chernyshev Bay is the presence of intensive NaCl crust within the littoral zone, where only thick-walled cysts of *Dunaliella* spp. can survive. Similar results were obtained by Heidelberg et al. (2013) during phytoplankton abundance analysis across hypersaline Lake Tyrrell, where they stated that *Dunaliella* spp. accounted for about 83% of the total identified phytoplankton organisms within the areas of high salt crust availability. Another reason may be the high concentration of *Artemia* that provided the nitrogen source enhancing the growth of the algae (Oren, 2014).

Secondly, the *Dunaliella* spp. group was not further classified to the species taxon; however, presumably, *Dunaliella salina* and *Dunaliella viridis* were some of the species present in the sample as they are usually a few of the most abundant algae found in waters with extreme salinity, such as the Great Salt Lake and Dead Sea, where it usually serves as the primary producer of a such ecosystem (Oren, 2014; Barteneva et al., 2019; Polle et al., 2020a; Polle et al., 2020b). The visual analysis of water images obtained during the Aral-2022 expedition supports the presence of *Dunaliella salina* and *Dunaliella viridis* due to the intensive blooming of Chernyshev Bay (Figure 4D). As seen, the water had the reddish color corresponding to the usual color of the β-carotene molecules that are extensively accumulated in the *Dunaliella* cells (Oren, 2014). In these lakes, the high salinity levels inhibit the growth of many phytoplankton organisms; however, *Dunaliella* spp. can tolerate such levels for exactly unknown mechanisms (Oren, 2014; Polle et al., 2020a). As a result, *Dunaliella* spp. are currently used as the model organism for the high salinity response, and there are a variety of ongoing transcriptome and proteome studies intended to find the mechanisms of tolerance (Oren, 2014; Polle et al., 2020a). For example, in the works of Chen et al. (2009), the glycerol-3-phosphate dehydrogenase (G3pgh) may be responsible for the tolerance mechanism. Another later work suggested that the system-to-salt response depend on the early and late responses and found a relation between some photosystem component (psaA, psaB, psbB, psbC), various chaperones (HSP70B, HSP90A) and ATP synthase subunits (atpA, atpB, atpE) to the salt stress regulation (Wang et al., 2019).

Lastly, several other phytoplankton genera were observed in the Chernyshev Bay, namely filamentous and biofilm cyanobacteria (e.g., *Aphanocapsa*), diatomic algae (*Aulacoseira* and non-identified diatoms), and *Pediastrum* genera (green algae). The presence of filamentous cyanobacteria was majorly described in studies of the Small Aral Sea, but no relevant data regarding the West Aral Sea and Chernyshev Bay (Orlova and Rusakova, 1999; Komárek, 2012; Klimaszyk et al., 2022). The existence of diatomic algae correlated with the studies of Barteneva et al. (2019), Bulatov (2021), and Plotnikov et al. (2023). Diatomic algae found in this study had the boat-shaped body type and presumably belonged to the *Navicula*

or *Nitzschia* genera; however, further analysis is needed (Barteneva et al., 2019; Guo et al., 2021; Khalil et al., 2021; Klimaszyk et al., 2022; Ruiz-Villarreal et al., 2022; Plotnikov et al., 2023). The presence of other genera is unique for the hypersaline lakes as they are most prevalent in freshwater.

4.3 NGS-based bacterioplankton taxonomy analysis

This study conducted a Nanopore-based 16S rRNA gene sequencing for the taxonomical analysis of bacterioplankton diversity of the Chernyshev Bay and the West Aral Sea. It was found that 4 genera, namely *Spiribacter*, *Halopeptonella*, *Halanaerobacter*, and *Salinibacter*, were the most abundant in Chernyshev Bay and accounted for more than 70% of total genera present. On the other hand, within the basin of the West Aral Sea, the most abundant genera were *Spiribacter*, *Halopeptonella*, and *Halomonas*. *Spiribacter* and *Halopeptonella* are the members of *Gammaproteobacteria* class and belong to the same family of *Ectothiorhodospiraceae* (Shurigin et al., 2019; León et al., 2020). *Halomonas* are also the members of *Gammaproteobacteria* class, however, it belongs to a different family called *Halomonadaceae* (Begmatov et al., 2020; Hu et al., 2021). Both littoral and limnetic zones of Chernyshev Bay had a high abundance of *Halanaerobacter* and *Salinibacter* which belong to classes *Halanaerobiia* and *Rhodothermata* respectively (Taroepratjeka et al, 2021; Viver et al., 2023). The above-mentioned prokaryotic genera were previously mentioned as the most abundant genera in the Aral Sea basin as well as other hypersaline water and soil reservoirs (Shurigin et al., 2019; Begmatov et al., 2020; León et al., 2020; Hu et al., 2021; Taroepratjeka et al., 2021; Viver et al., 2023). All of them are halophilic bacteria, however, the optimal level of salt concentration, pH, temperature and nutrients concentration differs across the species of each genera, and in order to compare the exact behavior of growth preferences, the classification up to the strain level is needed (Shurigin et al., 2019; Begmatov et al., 2020; León et al., 2020; Hu et al., 2021; Taroepratjeka et al, 2021; Viver et al., 2023).

These bacterioplankton genera are extensively studied for their potential roles in a variety of biogeochemical processes (e.g., arsenic cycling, sulfur cycling, and carbon fixation) (Paul et al., 2016; Edwardson and Hollibaugh, 2018). Besides, *Halomonas* spp. are extensively used for biotechnological purposes (e.g., production of amylases, cellulases, several dehydrogenases, and kinases) (Begmatov et al., 2020). Similarly, *Halanaerobacter* spp. are also used for the production of such materials as hydrogen and carbon dioxide gases, ethanol, formate, and lactate (Taroepratjeka et al., 2021).

The high concentrations of chitin producing *Artemia* spp that are extremely abundant in hypersaline lakes favored the interest in studies of chitinolytic bacterioplankton. This study also showed the presence of such bacterial genera as *Saccharospirillum* spp., *Arhodomonas* spp., and *Orenia* spp. in basins of the Chernyshev Bay and the West Aral Sea. *Saccharospirillum* spp. and *Arhodomonas* spp. were present in both regions, while *Orenia* was exclusively found in Chernyshev Bay. This difference can potentially be explained by the oxygen metabolism, where *Saccharospirillum* spp. and *Arhodomonas* spp. are aerobic bacteria and *Orenia* spp. anaerobic (Oren, 2015). Potentially the oxygen concentration in Chernyshev Bay favors the growth of Orenia spp. and of aerobic genera at lower levels. On the other hand, the West Aral Sea shows a high abundance of *Arhodomonas* spp. which may indicate the high oxygen availability in that region. Nevertheless, oxygen measurements are

required to confirm this correlation. The presence of chitinolytic bacteria was also confirmed in other hypersaline systems, for example, Lake Mono, the Great Salt Lake, the Dead Sea, soda lakes of Kulunda Steppe (Sorokin et al., 2012; Oren, 2015; Sorokin et al., 2016). The importance of these organisms comes from their role in the chitin degradation cycle and also their potential application in biotechnology and agriculture (Swiontek Brzezinska et al., 2013; Veliz et al., 2017; Edwardson and Hollibaugh, 2018).

In total, it is seen that in this study, the most abundant bacterioplankton genera within the West Aral Sea were represented by different genera of the same class *Gammaproteobacteria*, while higher taxonomical diversity was recorded in the samples of Chernyshev Bay. Nevertheless, WA2 had the highest number of genera compared to the other locations; oppositely WA1 had the lowest. Additionally, Shannon index analysis showed that higher values for the points from the West Aral Sea, which may indicate that it has higher bacterioplankton biodiversity compared to Chernyshev Bay. Besides NMDS test showed genera dissimilarities between Chernyshev Bay and the West Aral Sea. Comparing the littoral and limnetic zones of the Chernyshev Bay, the locations were represented close to each other on the NMDS graph, indicating the strong similarity among the littoral and limnetic zones. Also, it indicated the difference between the West Aral Sea's points among themselves, which may be because of the high difference in the total genera number. Additional studies are required to test whether there is such dissimilarity or not.

4.4 Statistical confirmation of hypothesis

The abovementioned hydrochemistry and taxonomical data were further correlated to test the hypothesis, which assumed that the distribution of phytoplankton and bacterioplankton communities differs among the Chernyshev Bay and the West Aral Sea. Considering the information gathered during both experimental stages and following analysis, the hypothesis was confirmed, and there are certain dissimilarities in phytoplankton and bacterioplankton diversities that are majorly influenced by conductivity and ammonium concentration.

4.5 Limitations

A variety of limiting sources occurred during this study. Firstly, in the hydrochemistry analysis, one of the major limitations was that all concentration measurements were conducted on the diluted samples. The necessity of this approach arises due to the high concentration of measured particles within the stock solution and the requirement to bring the concentration within the detectable ranges of the corresponding devices. Besides, depending upon the methodology, the desired ranges and, consequently the dilution factor was also different (e.g., for detectable ammonium range: $0 - 1.0$ mg/L N; nitrate detectable range: $0 - 20.0$ mg/L N; nitrite detectable range: $0 - 0.5$ mg/L N). In general, as there is an increase in the dilution factor, there is an increase in the error of measurement of the initial concentration (Chase and Hoel, 1975). Besides, the resulting solutions required different dilution factors for each test, which may differently impacted the potential error in measurements.

Secondly, IFC analysis was conducted on the samples that were taken under 10x magnification at autoimage mode. This mode generally provides a higher estimation of cell

abundances due to insufficient samplings (Dashkova et al., 2017). However, the nano- and microplankton image characterization was excluded from this study. An alternative solution may be the use of a fluorescence-triggered mode, where the scientist can narrow the image collection towards the organism of interest (Alvarez et al., 2013; Dashkova et al., 2017).. This limitation comes because IFC is a semi-automated method itself and potentially can be decreased as it moves towards more automated image analysis (Blaschko et al., 2005; Drews et al., 2013; Dashkova et al., 2017).

Next, during the NGS, there are several potential sources of limitations that can be categorized as follows: 1) Nanopore sequencing limitation and 2) database limitation. As stated above, Nanopore-based sequencing uses long reads, but the reading of electric signal during the sequencing is prone to the errors, which may influence the results (Winand et al., 2019; Egeter et al., 2022; Meirkhanova, 2022). Another limitation is the use of the SILVA (v. 138.1) database only. The problem lies in the necessity to constantly update it, which sometimes raises certain difficulties, like not having the opportunity to cultivate the species in the laboratory conditions or the absence of the species in the corresponding database (Malashenkov et al., 2021).

Chapter 5 – Conclusions and Future directions

In this research, we demonstrated the difference in the distribution of phytoplankton and bacterioplankton communities of Chernyshev Bay and West Aral Sea with the change in environmental variables. First of all, during the Aral-2022 expedition we observed the full separation of the Chernyshev Bay and the main waters of West Aral Sea. Secondly, the hydrochemistry analysis revealed a significant increase in conductivity and related salinity comparing for the results of the previous expeditions. Next, the developed methodology for IFC and NGS phytoplankton and bacterioplankton analysis was successfully applied for the characterization of the Chernyshev Bay and the West Aral Sea. The characterization of phytoplankton was conducted using the IFC approach at autoimage mode at 10x magnification. It showed that the *Dunaliella* spp was the dominant genus within the waters of Chernyshev Bay, accounting for more than 98% of total phytoplankton abundance, while its amounts were negligible or completely absent in the West Aral Sea. Nanopore-based NGS bacterioplankton analysis indicated that West Aral Sea had higher genera number compared to Chernyshev Bay. The 4 most abundant genera in the Chernyshev Bay are *Spiribacter* spp., *Halopeptonella* spp., *Halanaerobacter* spp., and *Salinibacter* spp. In the West Aral Sea, the situation was slightly different, where 3 most abundant genera are *Spiribacter* spp., *Halopeptonella* spp., and *Halomonas* spp. Additionally, the analysis showed the presence of chitin-degrading bacteria genera such as *Saccharospirillum* spp., *Arhodomonas* spp., and *Orenia* spp., potentially due to the presence of crustacean of the *Artemia* spp. Lastly, according to NMDS and PCA results conductivity and ammonium concentration were shown to be the most important parameters contributing to bacterioplankton dissimilarity among Chernyshev Bay and the West Aral Sea.

The future directions involve the use of new *in silico* based methods for IFC analysis, categorization of the data against other databases with the comparison of the resulting outputs, performing an additional test on the plankton dataset such as 18S rRNA sequencing, and

completion of full IFC and NGS analysis of Aral-2022 expedition samples which involves samples from different water depths.

Chapter 6 – Significance and applications

This research is the first work which used an NGS-based approach for the characterization of the bacterioplankton communities in Chernyshev Bay and has the potential to contribute to local and international limnology research.

From the local perspective, there are several studies performed on the Aral Sea, which primarily focused on the drying process, the changes in water basin levels, and its effect on salinity and temperature levels (Roget et al., 2009; Shi et al., 2014; Ayzel and Izhitskiy, 2018; Massakbayeva et al., 2020). For many years the primary focus in studies of Aral Sea biodiversity was focused on macroorganisms (Mirabdullayev et al., 2004; Micklin, 2016; Aladin et al., 2018). The interest in its microbiome has increased over the last decade, however, the major technology used for the analysis didn't involve sequencing (Sapozhnikov and Kalinina, 2019). Only in the last 5 years, there has been an increase in performing the analysis of the Aral Sea's microbiome using sequencing analysis. There are several studies obtained on several parts of the West Aral Sea, but the majority of them were performed on the territory of Uzbekistan, majorly involving the coastal soil samples and some water samples (Shurigin et al., 2019; Begmanov et al., 2020; Gao et al., 2021; Jing et al., 2021). Only one work was based on the description of the microbiome on the territory of Kazakhstan, but the sequencing was performed in the Small Aral Sea (Alexyuk et al., 2021). The current study substantially contributed to the data on water microbiome biodiversity of northern parts of the West Aral Sea.

Considering the fact that the West Aral Sea is a stratified and hypersaline lake, this study provided the information on the distribution and composition of multiple phytoplankton genera in the stratified parts of the Aral Sea along with several abiotic factors, such as temperature, conductivity, and pH gradients. Correlation between diversity and abiotic factors was obtained using statistical tools. NGS procedure allowed us to identify the presence of the smallest picoplankton and their relative composition within the ecosystem. Combining the IFC and the sequencing datasets with statistical analysis provided the opportunity to estimate the quality of water in hypersaline lakes. This will broaden the knowledge about the phytoplankton and bacterioplankton diversity of the Aral Sea.

From the international perspective, the Aral Sea has many similarities with other hypersaline lakes such as the Dead Sea, Lake Urmia, Lake Poopo, Lake Eyre, Lake Mead, lakes of Carpathian Basin, and Lake Chad (Oren et al., 2010; Ahmadi et al., 2016; Singh et al., 2016; Wurtsbaugh et al., 2017; Chaudhari et al., 2018; Karami 2018; Shurigin et al., 2019; Varotsos et al., 2020; Somogyi et al., 2022). This means that the research on the phytoplankton and bacterioplankton diversity may contribute to the current knowledge by providing new data about epilimnion genera of hypersaline lakes. Other hypersaline lakes of the world are also at high risk of disappearance, which means that the delivery of the current ecological situation of the Aral Sea may provoke people towards certain actions intended to solve such problems on their territory. Besides this research has described Nanopore-based studies that can provide quantitative data on genera diversity and their relative composition

in the endemic aquatic ecosystem. Also, being a relatively portable sequencing tool, Nanopore sequencing allows the seasonal monitoring of the Aral Sea and potentially other hypersaline lakes (Ahmadi et al., 2016; Yapiyev et al., 2017b; Chaudhari et al., 2018; Somogyi et al., 2022). This approach can be reproduced by other researchers across the globe to study their local lakes.

List of Tables

List of Figures

Abbreviations

DNA   deoxyribonucleic acid

IFC   imaging glow cytometry

NGS   next-generation sequencing

NMDS   non-metric multidimensional scaling

PCA   principal component analysis

PCR   polymerase chain reaction

Acknowledgments

Declaration

I declare that the research contained in this thesis, unless otherwise formally indicated within the text, is my original work. The thesis has been written by me its entirety. I duly acknowledged all sources of information which have been used in the thesis. The thesis has not been previously submitted to this or any other university for a degree and does not incorporate any material already submitted for a degree.

Signature: Date: 13/04/2023

Bibliography

Ahmadi A, Abbaspour M, Arjmandi R, Abedi Z. Resilient approach toward urban development in lake catchments, case of Urmia Lake. Scientia Iranica. 2016;23(4):1627–1632.

Aladin NV, Gontar VI, Zhakova LV, Plotnikov IS, Smurov AO, Rzymski P, et al. The zoocenosis of the Aral Sea: Six decades of fast-paced change. Environmental Science and Pollution Research. 2018;26(3):2228–2237.

Aladin NV, Høeg JT, Plotnikov I. Small Aral Sea brings hope for Lake Balkhash. Science. 2020;370(6522):1283.

Alexyuk M, Bogoyavlenskiy A, Alexyuk P, Moldakhanov Y, Berezin V, Digel I. Epipelagic microbiome of the small Aral Sea: Metagenomic structure and ecological diversity. Microbiology Open. 2020;10(1):e1142. doi: 10.1002/mbo3.1142.

Álvarez E, Moyano M, López-Urrutia Á, Nogueira E, Scharek R. Routine determination of plankton community composition and size structure: A comparison between Flowcam and light microscopy. Journal of Plankton Research. 2013;36(1):170–184.

Aminikhoei Z, Far EE, Taherpanah S, Samani MN. Assessment of flocculation induced by pH increase for harvesting microalgae Cyanothece sp. International Journal of Aquatic Biology. 2021; 9(5): 326-332.

Andrei A-Ş, Robeson MS, Baricz A, Coman C, Muntean V, Ionescu A, et al. Contrasting taxonomic stratification of microbial communities in two hypersaline meromictic lakes. The ISME Journal. 2015;9(12):2642–2656.

Arrigo KR. Marine microorganisms and global nutrient cycles. Nature. 2005;437(7057):349–355.

Aszalós JM, Szabó A, Megyes M, Anda D, Nagy B, Borsodi AK. Bacterial diversity of a high-altitude permafrost thaw pond located on Ojos del Salado (Dry Andes, Altiplano-Atacama Region). Astrobiology. 2020;20(6):754–765.

Ayzel G, Izhitskiy A. Coupling physically based and data-driven models for assessing freshwater inflow into the small Aral Sea. Proceedings of the International Association of Hydrological Sciences. 2018; 379:151–158.

Barteneva N, Dashkova V, Malashenkov D, Abilkas A, Zhantuyakova A, Baishulakova A, Sarkytbayev K, Abdimanova A, Samarkhanov K, Tulegenova N, Sadyrbayeva N, Vorobjev I, Voros L. Dramatic fluctuations in salinity and ecosystems of Aral Sea remnant bodies. Lakes&Reservoirs: Hot spots and topics in Lymnology. Mikorzyn, Poland. 2019.

Begmatov SA, Selitskaya OV, Vasileva LV, Berestovskaja YY, Manucharova NA, Drenova NV. Morphophysiological features of some cultivable bacteria from saline soils of the Aral Sea Region. Eurasian Soil Science. 2020;53(1):90–96.

Berard G, Applin D, Cloutis E, Stromberg J, Sharma R, Mann P, et al. A hypersaline spring analogue in Manitoba, Canada for potential ancient spring deposits on Mars. Icarus. 2013;224(2):399–412.

Berdimbetova GE, Orazova SS, Yuldasheva NK, Khidoyatova SK, Gusakova SD, Sagdullaev SS. Lipids from cysts of Aral sea brine shrimp *Artemia parthenogenetica*. Chemistry of Natural Compounds. 2019;55(5):802–805.

Blaschko MB, Holness G, Mattar MA, Lisin D, Utgoff PE, Hanson AR, et al. Automatic in situ identification of plankton. 2005 Seventh IEEE Workshops on Applications of Computer Vision (WACV/MOTION'05) - Volume 1. 2005;1:79-86.

Boehrer B, Schultze M. Stratification of lakes. Reviews of Geophysics. 2008;46(2). doi:10.1029/2006RG000210.

Breitwieser FP, Salzberg SL. Pavian: Interactive analysis of Metagenomics data for microbiome studies and Pathogen identification. Bioinformatics. 2019;36(4):1303–1304.

Bulatov SA. The diatom Flora (Bacillariophyta) of Kara-Bogaz-Gol Bay, the Caspian Sea: New data. Russian Journal of Marine Biology. 2021;47(4):265–273.

Buzgeia MH, Alhamali H, Nouh F, Elfagi S, Almanssi S. Study of the Physico-chemical Properties of Local and Imported Bottled Drinking Water in Benghazi and Their Compliance with the Libyan Specifications for Bottled Drinking water. European Journal of Business & Social Sciences. 2022;10(5).

Chang JJ, Ip YC, Bauman AG, Huang D. Minion-in-arms: Nanopore sequencing to expedite barcoding of specimen-rich macrofaunal samples from Autonomous Reef Monitoring Structures. Frontiers in Marine Science. 2020;7:448. doi: 10.3389/fmars.2020.00448.

Chase GR, Hoel DG. Serial dilutions: Error effects and optimal designs. Biometrika. 1975;62(2):329–334.

Chaudhari S, Felfelani F, Shin S, Pokhrel Y. Climate and anthropogenic contributions to the desiccation of the second largest saline lake in the twentieth century. Journal of Hydrology. 2018; 560:342–353.

Chen H, Jiang J-G, Wu G-H. Effects of salinity changes on the growth of Dunaliella Salina and its isozyme activities of glycerol-3-phosphate dehydrogenase. Journal of Agricultural and Food Chemistry. 2009;57(14):6178–82.

Chen J, McIlroy SE, Archana A, Baker DM, Panagiotou G. A pollution gradient contributes to the taxonomic, functional, and resistome diversity of microbial communities in marine sediments. Microbiome. 2019;7(1). https://doi.org/10.1186/s40168-019-0714-6.

Crétaux J-F, Kouraev AV, Papa F, Bergé-Nguyen M, Cazenave A, Aladin N, et al. Evolution of sea level of the Big Aral Sea from satellite altimetry and its implications for water balance. Journal of Great Lakes Research. 2005;31(4):520–534.

Dashkova V, Malashenkov D, Poulton N, Vorobjev I, Barteneva NS. Imaging flow cytometry for phytoplankton analysis. Methods. 2017;112:188–200.

Davidov K, Iankelevich-Kounio E, Yakovenko I, Koucherov Y, Rubin-Blum M, Oren M. Identification of plastic-associated species in the Mediterranean Sea using DNA metabarcoding with Nanopore minion. Scientific Reports. 2020;10(1). DOI: https://doi.org/10.1038/s41598-020-74180-z.

De Coster W, D'Hert S, Schultz DT, Cruts M, Van Broeckhoven C. NanoPack: Visualizing and processing long-read sequencing data. Bioinformatics. 2018;34(15):2666–2669.

Drews P, Colares RG, Machado P, de Faria M, Detoni A, Tavano V. Microalgae classification using semi-supervised and active learning based on gaussian mixture models. Journal of the Brazilian Computer Society. 2013;19(4):411–422.

Dutta J, Dutta J, Sen T, Zaman S, Mitra A. Influence of aquatic ph on dissolved PB in East Kolkata wetlands: A case study with reference to climate change induced acidification. Research Square. 2021. DOI: https://doi.org/10.21203/rs.3.rs-577162/v1.

Edwardson CF, Hollibaugh JT. Composition and activity of microbial communities along the redox gradient of an alkaline, hypersaline, Lake. Frontiers in Microbiology. 2018;9. DOI: https://doi.org/10.3389/fmicb.2018.00014.

Egeter B, Veríssimo J, Lopes-Lima M, Chaves C, Pinto J, Riccardi N, et al. Speeding up the detection of invasive bivalve species using environmental DNA: A Nanopore and Illumina sequencing comparison. Molecular Ecology Resources. 2022;22(6):2232–2247.

EPA. Method 365.1, Revision 2.0: Determination of Phosphorus by Semi-Automated Colorimetry. Ohio: U.S. Environmental Protection Agency; 1993.

Esenkulova S, Sutherland BJG, Tabata A, Haigh N, Pearce CM, Miller KM. Comparing metabarcoding and morphological approaches to identify phytoplankton taxa associated with harmful algal blooms. FACETS. 2020;5(1):784–811.

Franks PJ, Keafer BA. Sampling techniques and strategies for coastal phytoplankton blooms. Manual on marine microalgae. 2003.

Friedrich J, Oberhänsli H. Hydrochemical properties of the Aral Sea Water in summer 2002. Journal of Marine Systems. 2004;47(1-4):77–88.

Gao L, Ma J, Liu Y, Huang Y, Mohamad OA, Jiang H, et al. Diversity and biocontrol potential of cultivable endophytic bacteria associated with halophytes from the West Aral Sea Basin. Microorganisms. 2021;9(7):1448. doi: 10.3390/microorganisms9071448.

Guillard RL, Morton SL. Culture Methods. Manual on marine microalgae. 2003.

Guo J, Ma Y, Lee JHW. Real-time automated identification of algal bloom species for fisheries management in subtropical coastal waters. Journal of Hydro-environment Research. 2021;36:1–32.

Gupta N, Verma VK. Next-generation sequencing and its application: Empowering in public health beyond reality. Microorganisms for Sustainability. 2019;:313–41.

Heidelberg KB, Nelson WC, Holm JB, Eisenkolb N, Andrade K, Emerson JB. Characterization of eukaryotic microbial diversity in Hypersaline Lake Tyrrell, Australia. Frontiers in Microbiology. 2013;4. doi: 10.3389/fmicb.2013.00115.

Hosikian A, Lim S, Halim R, Danquah MK. Chlorophyll extraction from microalgae: A review on the process engineering aspects. International Journal of Chemical Engineering. 2010;2010:1–11.

Hrycik AR, Shambaugh A, Stockwell JD. Comparison of flowcam and microscope biovolume measurements for a diverse freshwater phytoplankton community. Journal of Plankton Research. 2019;41(6):849–864.

Hu J, Yan J, Wu L, Bao Y, Yu D, Li J. Simultaneous nitrification and denitrification of hypersaline wastewater by a robust bacterium Halomonas Salifodinae from a repeated-batch acclimation. Bioresource Technology. 2021;341:125818. DOI: https://doi.org/10.1016/j.biortech.2021.125818.

Izhitskaya ES, Egorov AV, Zavialov PO, Yakushev EV, Izhitskiy AS. Dissolved methane in the residual basins of the Aral Sea. Environmental Research Letters. 2019;14(6):065005. DOI 10.1088/1748-9326/ab0391.

Izhitskiy AS, Khymchenko EE, Zavialov PO, Serebryany AN. Hydrophysical State of the large Aral Sea in the autumn of 2013: Thermal structure, currents, and internal waves. Oceanology. 2014;54(4):414–425.

Izhitskiy AS, Zavialov PO, Sapozhnikov PV, Kirillin GB, Grossart HP, Kalinina OY, Zalota AK, Goncharenko IV, Kurbaniyazov AK. Present state of the Aral Sea: diverging physical and biological characteristics of the residual basins, Scientific Reports, 2016; 6, 23906. DOI: https://doi.org/10.1038/srep23906.

Jamshidi S, Bin Abu Bakar N. Variability of Dissolved Oxygen and Active Reaction in Deep Water of the Southern Caspian Sea, Near the Iranian Coast. Pol J Environ Stud. 2011;20(5):1167–80.

Jarsjö J, Destouni G. Groundwater discharge into the Aral Sea after 1960. Journal of Marine Systems. 2004;47(1-4):109–120.

Jiang H, Huang J, Li L, Huang L, Manzoor M, Yang J, et al. Onshore soil microbes and endophytes respond differently to geochemical and mineralogical changes in the Aral Sea. Science of The Total Environment. 2021; 765:142675. DOI: 10.1016/j.scitotenv.2020.142675.

Karami N. The Drying of Lake Urmia as a Case of the "Aralism" Concept in Totalitarian Systems. International Journal of Geography and Regional Planning. 2018; 4(1):43-63.

Khalil S, Mahnashi MH, Hussain M, Zafar N, Waqar-Un-Nisa, Khan FS, et al. Exploration and determination of algal role as bioindicator to evaluate water quality – probing fresh water algae. Saudi Journal of Biological Sciences. 2021;28(10):5728–5737.

Klimaszyk P, Kuczyńska-Kippen N, Szeląg-Wasielewska E, Marszelewski W, Borowiak D, Niedzielski P, et al. Spatial heterogeneity of chemistry of the small Aral Sea and the syr darya river and its impact on plankton communities. Chemosphere. 2022;307:135788. DOI: https://doi.org/10.1016/j.chemosphere.2022.135788.

Komárek J. Nomenclatural changes in heterocytous Cyanoprokaryotes (Cyanobacteria, Cyanophytes). Fottea. 2012;12(1):141–148.

Koren S, Walenz BP, Berlin K, Miller JR, Bergman NH, Phillippy AM. Canu: Scalable and accurate long-read assembly via adaptive k-mer weighting and repeat separation. Genome Res. 201; 27:722–736.

León MJ, Galisteo C, Ventosa A, Sánchez-Porro C. *Spiribacter aquaticus* Leon et al. 2017 is a later heterotypic synonym of *Spiribacter roseus* Leon et al. 2016. reclassification of *Halopeptonella vilamensis* Menes et al. 2016 as *Spiribacter vilamensis* comb. Nov.. International Journal of Systematic and Evolutionary Microbiology. 2020;70(4):2873–2878.

Lu J, Rincon N, Wood DE, Breitwieser FP, Pockrandt C, Langmead B, et al. Metagenome analysis using the Kraken Software Suite. Nature Protocols. 2022. DOI: https://doi.org/10.1038/s41596-022-00738-y.

Madsen EL. Microorganisms and their roles in fundamental biogeochemical cycles. Current Opinion in Biotechnology. 2011;22(3):456–464.

Makaya E, Zuvarinopisa A. Application of Peanut Shell Activated Carbon in Drinking Water Treatment. International Journal of Environmental Pollution and Nutrient Cycling. 2019;1(1).

Makkaveev PN, Gordeev VV, Zav'yalov PO, Polukhin AA, Khlebopashev PV, Kochenkova AI. Hydrochemical characteristics of the Aral Sea in 2012–2013. Water Resources. 2018;45(2):188–198.

Malashenkov DV, Dashkova V, Zhakupova K, Vorobjev IA, Barteneva NS. Comparative analysis of freshwater phytoplankton communities in two lakes of Burabay National Park using morphological and molecular approaches. Scientific Reports. 2021;11(1). doi: 10.1038/s41598-021-95223-z.

Marden B, Brown P, Bosteels T. Great Salt Lake artemia: Ecosystem functions and services with a global reach. Great Salt Lake Biology. 2020;:175–237.

Massakbayeva A, Abuduwaili J, Bissenbayeva S, Issina B, Smanov Z. Water balance of the small Aral Sea. Environmental Earth Sciences. 2020;79(3):1–11.

Mavzhudova AM, Mamarasulov BD, Tonkikh AK, Husanov TS. Manufacturing features of *Dunaliella salina* AR-1 and the influence of soles on the application of β-carotins. European Journal of Molecular & Clinical Medicine. 2020;7(2): 2194–2203.

Meirkhanova A. Next-generation sequencing for studying microbial communities during cyanobacterial algal blooms. Thesis, Astana. 2022.

Micklin, PP. Desiccation of the aral sea: a water management disaster in the Soviet Union. Science, 1988; 241, 1170–1176.

Micklin P. The Aral Sea Disaster. Annu. Rev. Earth Planet. Sc., 2007; 35, 47–72.

Micklin P. The future Aral Sea: Hope and despair. Environmental Earth Sciences. 2016;75(9). DOI: https://doi.org/10.1007/s12665-016-5614-5.

Mirabdullayev IM, Joldasova IM, Mustafaeva ZA, Kazakhbaev S, Lyubimova SA, Tashmukhamedov BA. Succession of the ecosystems of the Aral Sea during its transition from oligohaline to polyhaline water body. Journal of Marine Systems. 2004;47(1-4):101–107.

Mirasbekov Y, Abdimanova A, Sarkytbayev K, Samarkhanov K, Abilkas A, Potashnikova D, et al. Combining imaging flow cytometry and molecular biological methods to

reveal presence of potentially toxic algae at the Ural River in Kazakhstan. Frontiers in Marine Science. 2021;8:680482. doi: 10.3389/fmars.2021.680482.

Mirzahasanlou JP, Hejazi MA. Effect of CO2 on growth parameters and lipid production in *Dunaliella* sp.. ABRIINW-I1 (Chlorophyceae) isolated from Urmia Lake, NW Iran. 2022; ResearchSquare. DOI: https://doi.org/10.21203/rs.3.rs-1632443/v1.

Nygaard AB, Tunsjø HS, Meisal R, Charnock C. A preliminary study on the potential of Nanopore minion and Illumina Miseq 16S rrna gene sequencing to characterize building-dust microbiomes. Scientific Reports. 2020;10(1). DOI: https://doi.org/10.1038/s41598-020-59771-0.

Oberhänsli H, Boroffka N, Sorrel P, Krivonogov S. Climate variability during the past 2,000 years and past economic and irrigation activities in the Aral Sea Basin. Irrigation and Drainage Systems. 2007;21(3-4):167–183.

Oren A, Plotnikov IS, Sokolov S, Aladin NV. The Aral Sea and the Dead Sea: Disparate lakes with similar histories. Lakes & Reservoirs: Science, Policy and Management for Sustainable Use. 2010;15(3):223–236.

Oren A. Halophilic microbial communities and their environments. Current Opinion in Biotechnology. 2015;33:119–24.

Oren A. The ecology of *Dunaliella* in high-salt environments. Journal of Biological Research-Thessaloniki. 2014;21(1). DOI: https://doi.org/10.1186/s40709-014-0023-y.

Orlova MI, Rusakova OM. Characteristics of coastal phytoplankton near Cape Tastubec (northern Aral Sea). International Journal of Salt Lake Research. 1999;8(1):7–18.

Paul D, Kumbhare SV, Mhatre SS, Chowdhury SP, Shetty SA, Marathe NP, et al. Exploration of microbial diversity and community structure of Lonar Lake: The only hypersaline Meteorite Crater Lake within Basalt Rock. Frontiers in Microbiology. 2016;6. DOI: https://doi.org/10.3389/fmicb.2015.01553.

Pichler M, Coskun ÖK, Ortega-Arbulú AS, Conci N, Wörheide G, Vargas S, et al. A 16S rRNA gene sequencing and analysis protocol for the Illumina MiniSeq platform. MicrobiologyOpen. 2018;7(6). DOI: https://doi.org/10.1002/mbo3.611.

Plotnikov IS, Aladin NV, Zhakova LV, Mossin J, Høeg JT. Past, Present and Future of the Aral Sea - A Review of its Fauna and Flora before and during the Regression Crisis . Zoological Studies. 2023;62(19).

Plotnikov IS, Ermakhanov ZK, Aladin NV, Micklin P. Modern state of the Small (Northern) aral sea fauna. Lakes & Reservoirs: Science, Policy and Management for Sustainable Use. 2016;21(4):315–328.

Polle JEW, Jin ES, Ben-Amotz A. The Alga *Dunaliella* Revisited: Looking back and moving forward with model and production organisms. Algal Research. 2020a;49:101948. DOI: https://doi.org/10.1016/j.algal.2020.101948.

Polle JEW, Roth R, Ben-Amotz A, Goodenough U. Ultrastructure of the green alga *Dunaliella salina* strain CCAP19/18 (Chlorophyta) as investigated by quick-freeze deep-etch electron microscopy. Algal Research. 2020b;49:101953. DOI: https://doi.org/10.1016/j.algal.2020.101953.

Raskin P, Hansen E, Zhu Z, Stavisky D. Simulation of Water Supply and Demand in the Aral Sea Region. Water Int., 1992; 17, 55–67.

Raveh A, Avnimelech Y. Total nitrogen analysis in water, soil and plant material with persulphate oxidation. Water Research. 1979;13(9):911–912.

Reed JM, Mesquita-Joanes F, Griffiths HI. Multi-indicator conductivity transfer functions for quaternary palaeoclimate reconstruction. Journal of Paleolimnology. 2012;47(2):251–275.

Roget E, Zavialov P, Khan V, Muñiz MA. Geodynamical processes in the channel connecting the two lobes of the large Aral Sea. Hydrology and Earth System Sciences. 2009;13(11):2265–2271.

Ruiz-Villarreal M, Sourisseau M, Anderson P, Cusack C, Neira P, Silke J, et al. Novel methodologies for providing in situ data to Hab early warning systems in the European Atlantic Area: The Primrose Experience. Frontiers in Marine Science. 2022;9. DOI: https://doi.org/10.3389/fmars.2022.791329.

Salazar G, Sunagawa S. Marine Microbial Diversity. Current Biology. 2017;27(11): R489–R494.

Salmi P, Eskelinen MA, Leppänen MT, Pölönen I. Rapid quantification of microalgae growth with hyperspectral camera and vegetation indices. Plants. 2021;10(2):341. DOI: https://doi.org/10.3390/plants10020341.

Sapozhnikov P, Kalinina O. Main results of observations of changes in bottom biota and ichthyofauna of the Large Aral Sea in the period 2002–2017. Ecology of hydrosphere, 2019. DOI: 10.33624/2587-9367-2018-1(2)-41-54. [RUS].

Sellner KG, Doucette GJ, Kirkpatrick GJ. Harmful algal blooms: Causes, impacts and detection. Journal of Industrial Microbiology and Biotechnology. 2003;30(7):383–406.

Small EE, Sloan LC, Nychka D. Changes in surface air temperature caused by desiccation of the Aral Sea. J. Climate, 2001; 14(3), 284–299.

Shi W, Wang M, Guo W. Long-term hydrological changes of the Aral Sea observed by satellites. Journal of Geophysical Research: Oceans. 2014;119(6):3313–3326.

Shurigin V, Hakobyan A, Panosyan H, Egamberdieva D, Davranov K, Birkeland NK. A glimpse of the prokaryotic diversity of the large Aral Sea reveals novel extremophilic bacterial and Archaeal Groups. MicrobiologyOpen. 2019;8(9). DOI: https://doi.org/10.1002/mbo3.850.

Singh A, Seitz F, Eicker A, Güntner A. Water budget analysis within the surrounding of prominent lakes and reservoirs from multi-sensor Earth observation data and hydrological models: Case studies of the Aral Sea and lake mead. Remote Sensing. 2016;8(11):953. DOI: https://doi.org/10.3390/rs8110953.

Singh A, Seitz F, Schwatke C. Inter-annual water storage changes in the Aral Sea from multi-mission satellite altimetry, optical remote sensing, and Grace Satellite Gravimetry. Remote Sensing of Environment. 2012; 123:187–195.

Somogyi B, Felföldi T, Boros E, Szabó A, Vörös L. Where the little ones play the main role—Picophytoplankton predominance in the soda and hypersaline lakes of the Carpathian Basin. Microorganisms. 2022;10(4):818. DOI: 10.3390/microorganisms10040818.

Sorokin DY, Berben T, Melton ED, Overmars L, Vavourakis CD, Muyzer G. Microbial diversity and biogeochemical cycling in Soda Lakes. Extremophiles. 2014;18(5):791–809.

Sorokin DY, Rakitin AL, Gumerov VM, Beletsky AV, Sinninghe Damsté JS, Mardanov AV, et al. Phenotypic and genomic properties of Chitinispirillum alkaliphilum gen. Nov., sp. nov., a haloalkaliphilic anaerobic chitinolytic bacterium representing a novel class in the phylum fibrobacteres. Frontiers in Microbiology. 2016;7. doi: 10.3389/fmicb.2016.00407.

Sorokin DY, Tourova TP, Sukhacheva MV, Mardanov AV, Ravin NV. Bacterial chitin utilisation at extremely haloalkaline conditions. Extremophiles. 2012;16(6):883–94.

Stauffer BA, Bowers HA, Buckley E, Davis TW, Johengen TH, Kudela R, et al. Considerations in harmful algal bloom research and monitoring: Perspectives from a consensus-building workshop and Technology Testing. Frontiers in Marine Science. 2019;6. DOI: https://doi.org/10.3389/fmars.2019.00399.

Stunzhas PA. Calculation of electric conductivity of water of the Aral Sea and correction of the sound salinity of 2002–2009. Oceanology. 2016;56(6):782–788.

Swiontek Brzezinska M, Jankiewicz U, Burkowska A, Walczak M. Chitinolytic microorganisms and their possible application in environmental protection. Current Microbiology. 2013;68(1):71–81.

Szabó, A., Korponai, K., Kerepesi, C., Somogyi, B., Vörös, L., Bartha, D., Márialigeti, K. and Felföldi, T., 2017. Soda pans of the Pannonian steppe harbor unique bacterial communities adapted to multiple extreme conditions. *Extremophiles*, *21*(3), pp.639-649.

Taroepratjeka DA, Imai T, Chairattanamanokorn P, Reungsang A. Extremely halophilic biohydrogen producing microbial communities from high-salinity soil and salt evaporation pond. Fuels. 2021;2(2):241–252.

Utemuratova FJ, Kim SI, Kamilov BG, Yuldashov MA, Mustafaeva ZA. Biometrical study of Artemia cysts harvested from the aral sea in Uzbekistan. IOP Conference Series: Earth and Environmental Science. 2022;1068(1):012030. DOI: 10.1088/1755-1315/1068/1/012030.

Varotsos CA, Krapivin VF, Mkrtchyan FA. On the recovery of the water balance. Water, Air, & Soil Pollution. 2020;231(4). DOI: https://doi.org/10.1007/s11270-020-04554-6.

Veliz E, Martínez-Hidalgo P, M. Hirsch A. Chitinase-producing bacteria and their role in Biocontrol. AIMS Microbiology. 2017;3(3):689–705.

Verde C, Giordano D, Bellas CM, di Prisco G, Anesio AM. Polar Marine microorganisms and climate change. Advances in Microbial Physiology. 2016;:187–215.

Viver T, Conrad RE, Lucio M, Harir M, Urdiain M, Gago JF, et al. Description of two cultivated and two uncultivated new Salinibacter species, one named following the rules of the Bacteriological Code: Salinibacter grassmerensis sp. nov.; and three

named following the rules of the seqcode: Salinibacter Pepae sp. nov., Salinibacter Abyssi sp. nov., and Salinibacter Pampae sp. nov.. Systematic and Applied Microbiology. 2023;46(3):126416. DOI: 10.1016/j.syapm.2023.126416.

Wang Y, Cong Y, Wang Y, Guo Z, Yue J, Xing Z, et al. Identification of early salinity stress-responsive proteins in Dunaliella salina by isobaric tags for relative and absolute quantitation (itraq)-based quantitative proteomic analysis. International Journal of Molecular Sciences. 2019;20(3):599. doi: 10.3390/ijms20030599.

Warren CR. Rapid measurement of chlorophylls with a microplate reader. Journal of Plant Nutrition. 2008;31(7):1321–1332.

Werner D, Acharya K, Blackburn A, Zan R, Plaimart J, Allen B, et al. Minion Nanopore sequencing accelerates progress towards ubiquitous genetics in water research. Water. 2022;14(16):2491. DOI: https://doi.org/10.3390/w14162491.

Winand R, Bogaerts B, Hoffman S, Lefevre L, Delvoye M, Van Braekel J, et al. Targeting the 16S rna gene for bacterial identification in complex mixed samples: Comparative evaluation of second (Illumina) and third (Oxford Nanopore Technologies) generation sequencing technologies. International Journal of Molecular Sciences. 2019;21(1):298. doi: 10.3390/ijms21010298.

Wood DE, Lu J, Langmead B. Improved metagenomic analysis with Kraken 2. Genome Biology. 2019;20(1). DOI: https://doi.org/10.1186/s13059-019-1891-0.

Wurtsbaugh WA, Miller C, Null SE, DeRose RJ, Wilcock P, Hahnenberger M, et al. Decline of the world's Saline Lakes. Nature Geoscience. 2017;10(11):816–821.

Yang J, Ma L, Jiang H, Wu G, Dong H. Salinity shapes microbial diversity and community structure in surface sediments of the Qinghai-Tibetan Lakes. Scientific Reports. 2016;6(1). DOI: https://doi.org/10.1038/srep25078.

Yapiyev V, Sagintayev Z, Inglezakis V, Samarkhanov K, Verhoef A. Essentials of endorheic basins and lakes: A review in the context of current and future water resource management and mitigation activities in Central Asia. Water. 2017a;9(10):798. DOI: https://doi.org/10.3390/w9100798.

Yapiyev V, Sagintayev Z, Verhoef A, Kassymbekova A, Baigaliyeva M, Zhumabayev D, et al. The Changing Water Cycle: Burabay National Nature Park, Northern Kazakhstan. Wiley Interdisciplinary Reviews: Water. 2017b;4(5). DOI: https://doi.org/10.1002/wat2.1227.

Zavialov PO, Kostianoy AG, Emelianov SV, Ni AA, Ishniyazov D, Khan VM, Kudyshkin TV. Hydrographic survey in the dying Aral Sea. Geophys. Res. Lett. 2003; 30 (13), 1659. DOI: https://doi.org/10.1029/2003GL017427.

Zavialov P. Physical Oceanography of the Large Aral Sea. In: Kostianoy A, editor, Kosarev A, editor. The Aral Sea Environment The Handbook of Environmental Chemistry. Berlin, Heidelberg: Springer; 2010. p. 123–45.

Zeglin LH. Stream microbial diversity in response to environmental changes: Review and synthesis of existing research. Frontiers in Microbiology. 2015;6. DOI: https://doi.org/10.3389/fmicb.2015.00454.

Appendix 1 – Protocol links

Method name:	Link:
Phosphorous content analysis	https://www.epa.gov/sites/default/files/2015-08/documents/method_365-1_1993.pdf
Nitrogen content analysis	https://www.ysi.com/File%20Library/Documents/Manuals/YPT282-9300-9500-manual-with-test-procedures.pdf
DNA extraction	https://www.qiagen.com/kz/resources/resourcedetail?id=58f43d7e-172a-4970-84f0-9cb335a8d262&lang=en
Library construction	https://community.nanoporetech.com/docs/prepare/library_prep_protocols/16S-barcoding-1-24/v/16s_9086_v1_revx_14aug2019/library-preparation-16s?devices=minion *
Sequencing	https://community.nanoporetech.com/docs/prepare/library_prep_protocols/16S-barcoding-1-24/v/16s_9086_v1_revx_14aug2019/priming-and-loading-the-sp?devices=minion *

* - requires community account to access the protocol

Appendix 2 – Summary of reagents and resources

REAGENT or RESOURCE	SOURCE	IDENTIFIER
Sample Collection		
Multimeter Extech EC400	FLIR® Systems, Inc.	N/A
Glutaraldehyde Solution	Merck KGaA, Germany	340855
Liquid Nitrogen Vessel	N/A	N/A
Whatman® glass microfiber filters	Merck KGaA, Germany	WHA2822-047
Corning® 50 mL centrifuge tubes	Merck KGaA, Germany	CLS430291
Smart2Pure Water Purification System	Thermo Fisher Scientific, USA	Catalog No: 50129688
Ultrapure Water	N/A	N/A
Manual Vacuum Pump	N/A	N/A
Hydrochemistry: Phosphorous Content Analysis		
Corning® 50 mL centrifuge tubes	Merck KGaA, Germany	CLS430291
Potassium peroxidisulphate ($K_2S_2O_8$)	Merck KGaA, Germany	60489-250G-F
conc. Sulphuric Acid (H_2SO_4)	Merck KGaA, Germany	339741
Smart2Pure Water Purification System	Thermo Fisher Scientific, USA	Catalog No: 50129688
Ultrapure Water	N/A	N/A
Ascorbic Acid ($C_6H_8O_6$)	Merck KGaA, Germany	A92902
Ammonium heptamolybdate (($NH_4)_6Mo_7O_{24}$)	Merck KGaA, Germany	M1019
Potassium antimony (III) oxide tartrate ($K_2(SbO)_2C_8H_4O_{10}$)	Merck KGaA, Germany	244791
Potassium dihydrogen phosphate (KH_2PO_4)	Merck KGaA, Germany	P5655
conc. Sodium Hydroxide (NaOH)	Merck KGaA, Germany	S5881
Pyrex® glass culture tubes	Merck KGaA, Germany	Z653586
Eppendorf Research® plus (100 – 1000 µL)	Eppendorf Ltd., UK	Catalog No: 0030000927
Eppendorf Research® plus (20 – 200 µL)	Eppendorf Ltd., UK	Catalog No: 3123000055
epT.I.P.S.® Standard (50 – 1000 µL)	Eppendorf Ltd., UK	Catalog No: 0030000870
epT.I.P.S.® Standard (2 – 200 µL)	Eppendorf Ltd., UK	Catalog No: 0030000870
BRAND® glass beaker with spout, low form	Merck KGaA, Germany	BR91236-10EA
Evolution 300 UV-Vis Spectrophotometer	Thermo Fisher Scientific, USA	N/A
Hydrochemistry: Nitrogen Content Analysis		
Corning® 50 mL centrifuge tubes	Merck KGaA, Germany	CLS430291
Smart2Pure Water Purification System	Thermo Fisher Scientific, USA	Catalog No: 50129688
Ultrapure Water	N/A	N/A
YSI Photometer 9500	YSI, USA	discontinued
YSI Ammonium Test Kit	YSI, USA	discontinued
YSI Nitrate Test Kit	YSI, USA	discontinued
YSI Nitrite Test Kit	YSI, USA	discontinued
Eppendorf Research® plus (100–1000 µL)	Eppendorf Ltd., UK	Catalog No: 0030000927
Eppendorf Research® plus (20–200 µL)	Eppendorf Ltd., UK	Catalog No: 3123000055
epT.I.P.S.® Standard (50 – 1000 µL)	Eppendorf Ltd., UK	Catalog No: 0030000870
epT.I.P.S.® Standard (2 – 200 µL)	Eppendorf Ltd., UK	Catalog No: 0030000870
BRAND® glass beaker with spout, low form	Merck KGaA, Germany	BR91236-10EA
IEC Medilite Microcentrifuge	Thermo Fisher Scientific, USA	Catalog No: 004580F

IFC analysis		
Corning® 50 mL centrifuge tubes	Merck KGaA, Germany	CLS430291
FlowCAM	Yokogawa Fluid Imaging Technologies, USA	discontinued
VisualSpreadsheet	Yokogawa Fluid Imaging Technologies, USA	N/A
NGS: DNA Extraction		
Whatman® glass microfiber filters	Merck KGaA, Germany	WHA2822-047
DNEasy Power Water Kit	QIAGEN, Germany	ID: 14900–100-NF
Nanodrop	Thermo Fisher Scientific, USA	Catalog No: ND-8000-GL
Eppendorf Research® plus (20–200 µL)	Eppendorf Ltd., UK	Catalog No: 3123000055
Eppendorf Research® plus (0.5–10 µL)	Eppendorf Ltd., UK	Catalog No: 3123000020
Eppendorf Research® plus (0.1–2.5 µL)	Eppendorf Ltd., UK	Catalog No: 3123000012
epT.I.P.S.® Standard (2 – 200 µL)	Eppendorf Ltd., UK	Catalog No: 0030000870
epT.I.P.S.® Standard (0.1 – 20 µL)	Eppendorf Ltd., UK	Catalog No: 0030000838
Eppendorf Safe-Lock Tubes	Eppendorf Ltd., UK	Catalog No. 0030120086
NGS: Library Construction		
16S Barcoding Kit	Oxford Nanopore Technologies, UK	SQK-16S024
AMPure XP Beads	Beckman Coulter, USA	A63881
Thermocycler	Eppendorf Ltd., UK	Catalog No: 6331000041
DreamTaq™ Hot Start DNA Polymerase	Thermo Fisher Scientific, USA	EP1701
0.2 ml PCR Tubes	Bio-Rad Laboratories, Inc., USA	TFI0201
Eppendorf Research® plus (20–200 µL)	Eppendorf Ltd., UK	Catalog No: 3123000055
Eppendorf Research® plus (0.5–10 µL)	Eppendorf Ltd., UK	Catalog No: 3123000020
Eppendorf Research® plus (0.1–2.5 µL)	Eppendorf Ltd., UK	Catalog No: 3123000012
epT.I.P.S.® Standard (2 – 200 µL)	Eppendorf Ltd., UK	Catalog No: 0030000870
epT.I.P.S.® Standard (0.1 – 20 µL)	Eppendorf Ltd., UK	Catalog No: 0030000838
Eppendorf Safe-Lock Tubes	Eppendorf Ltd., UK	Catalog No: 0030120086
NGS: Sequencing		
MinION Mk1C Device	Oxford Nanopore Technologies, UK	MIN-101C
Flow Cell	Oxford Nanopore Technologies, UK	FLO-MIN106D
Flow Cell priming kit	Oxford Nanopore Technologies, UK	EXP-FLP002
Eppendorf Research® plus (0.5–10 µL)	Eppendorf Ltd., UK	Catalog No: 3123000020
Eppendorf Research® plus (0.1–2.5 µL)	Eppendorf Ltd., UK	Catalog No: 3123000012
epT.I.P.S.® Standard (0.1 – 20 µL)	Eppendorf Ltd., UK	Catalog No: 0030000838
NGS: Raw Data Analysis		

Guppy	Oxford Nanopore Technologies, UK	N/A
NanoPlot	De Coster et al., 2018	https://github.com/wdecoster/NanoPlot
Kraken2	Wood et al., 2019	https://github.com/DerrickWood/kraken2
Bracken	Wood et al., 2019	https://github.com/jenniferlu717/Bracken
Vegan R	N/A	https://github.com/vegandevs/vegan
Pavian	Breitwieser and Salzberg, 2020	https://github.com/fbreitwieser/pavian
NGS: Statistical Analysis		
Vegan R	N/A	https://github.com/vegandevs/vegan
PRIMER-7	PRIMER-e, New Zealand	https://www.primer-e.com/our-software/primer-version-7/

Appendix 3 – Supplementary tables

Table S1. Hydrochemistry raw data. Samples were diluted for several test: 1) DF of x40 was used for Conductivity, TDS, Salinity, Nitrate concentration, and Ammonium concentration measurements; 2) DF of x2 was used for Total phosphorous concentration, and Nitrite concentration measurements. The samples were not diluted during the pH and temperature measurements.

	pH:	Temperature (°C)	Conductivity (mS/cm):	Total phosphorous (mg/L):	Nitrite (mg/L):	Nitrate (mg/L):	Ammonium (mg/L):
CH_LIM_1	7.10	11.5	179.4	0.314	0.00	0.151	0.67
CH_LIM_2	7.26	14.4	189.0	0.313	0.00	0.000	0.50
CH_LIM_3	7.65	15.1	197.0	0.301	0.00	0.000	0.74
CH_LIM_4	7.55	14.5	191.0	0.292	0.01	0.020	0.92
CH_LIM_5	7.53	14.9	191.7	0.298	0.00	0.000	0.80
CH_LIM_6	7.55	15.1	192.7	0.251	0.00	0.000	0.86
CH_LIM_7	7.47	15.4	195.6	0.188	0.00	0.000	1.02
CH_LIT_1	7.20	13.0	106.5	0.290	0.00	0.000	0.79

CH_LIT_2	7.45	21.6	195.1	0.168	0.00	0.000	1.03
CH_LIT_3	7.41	21.6	190.3	0.329	0.00	0.000	0.84
CH_LIT_4	7.52	19.1	194.4	0.194	0.01	0.000	0.93
WA1	7.69	13.4	182.1	0.054	0.00	0.000	0.63
WA2	7.75	12.4	181.2	0.174	0.00	0.000	0.67

Table S2. The Nanodrop measurements of DNA concentration during NGS stage.

	DNA concentration after DNA extraction:	DNA concentration after PCR amplification:	DNA concentration after PCR product purification:
LIM 1	15.79 ng/µL	246.2 ng/ µL	1.09 ng/ µL
LIM 2	24.12 ng/ µL	326.4 ng/ µL	19.70 ng/ µL
LIM 3	23.39 ng/ µL	341.5 ng/ µL	8.48 ng/ µL
LIM 4	37.79 ng/ µL	305.4 ng/ µL	28.83 ng/ µL
LIM 5	45.93 ng/ µL	545.6 ng/ µL	13.76 ng/ µL
LIM 6	34.17 ng/ µL	527.8 ng/ µL	11.33 ng/ µL
LIM 7	57.53 ng/ µL	496.3 ng/ µL	7.57 ng/ µL
LIT 1	49.60 ng/ µL	871.8 ng/ µL	47.69 ng/ µL

LIT 2	14.37 ng/ µL	573.6 ng/ µL	23.72 ng/ µL
LIT 3	23.28 ng/ µL	305.5 ng/ µL	15.34 ng/ µL
LIT 4	17.20 ng/ µL	556.9 ng/ µL	4.03 ng/ µL
LIT 5	0.22 ng/ µL	529.1 ng/ µL	2.42 ng/ µL
LIT 6	2.82 ng/ µL	501.7 ng/ µL	7.32 ng/ µL

Appendix 4 – Supplementary figures
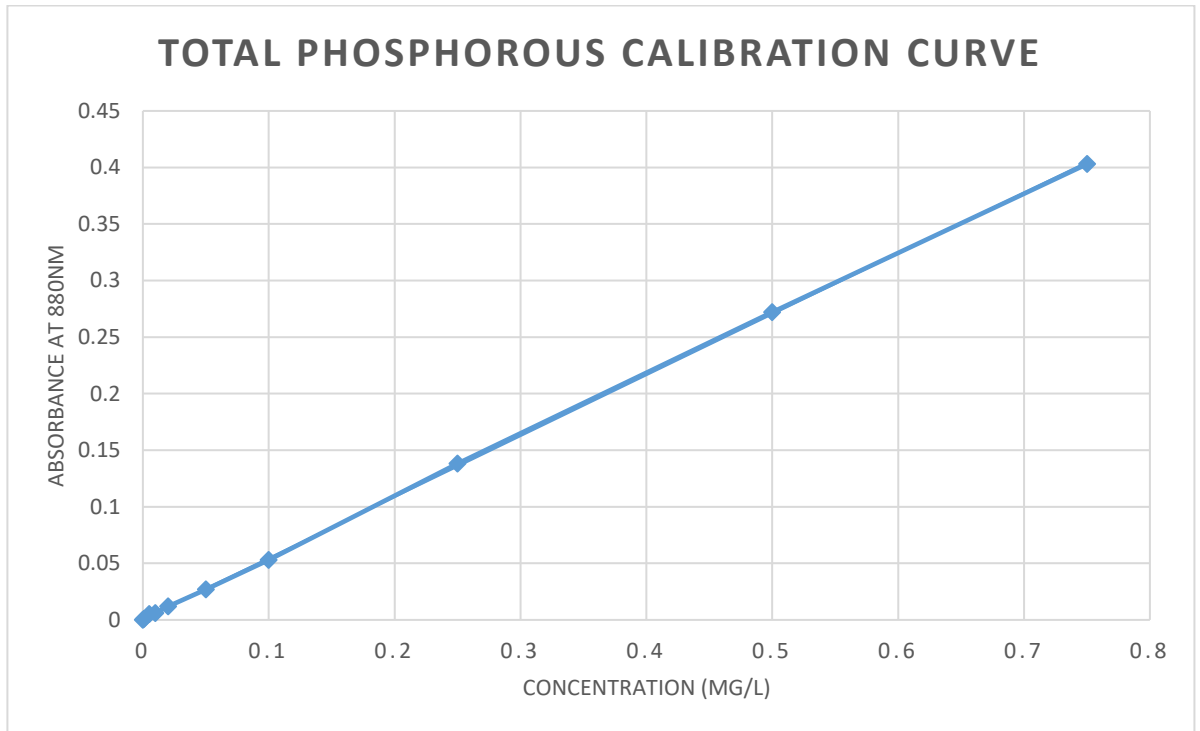

TOTAL PHOSPHOROUS CALIBRATION CURVE

Figure S1. Calibration curve was used for the Total phosphorous content analysis for Evolution 300 spectrophotometer.
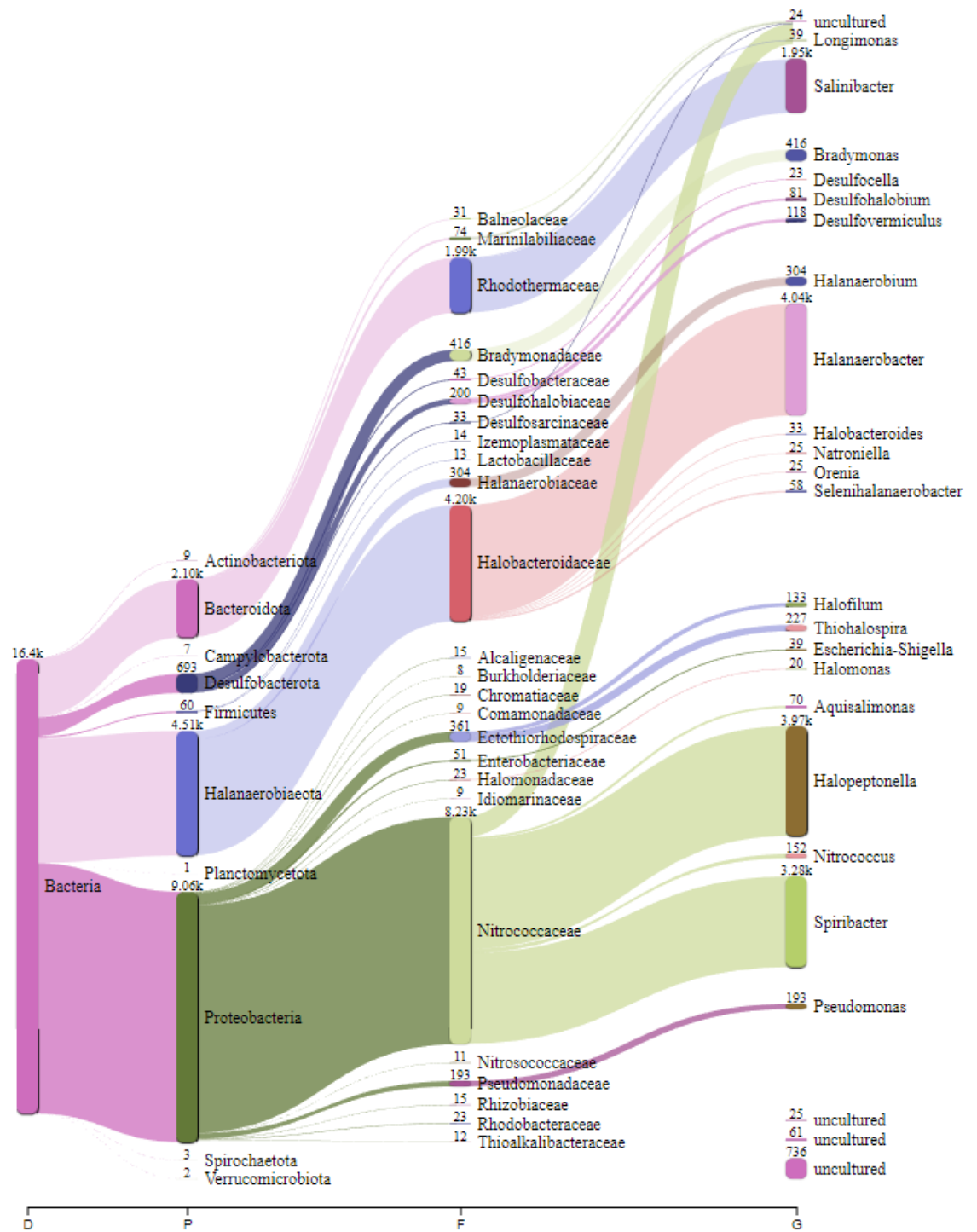
Figure S2. An example (CH_LIT_1) of phylogenetic analysis of the most abundant genera in the Chernyshev Bay's littoral zone.

Figure S3. An example (CH_LIM_1) of phylogenetic analysis of the most abundant genera in the Chernyshev Bay's limnetic zone.
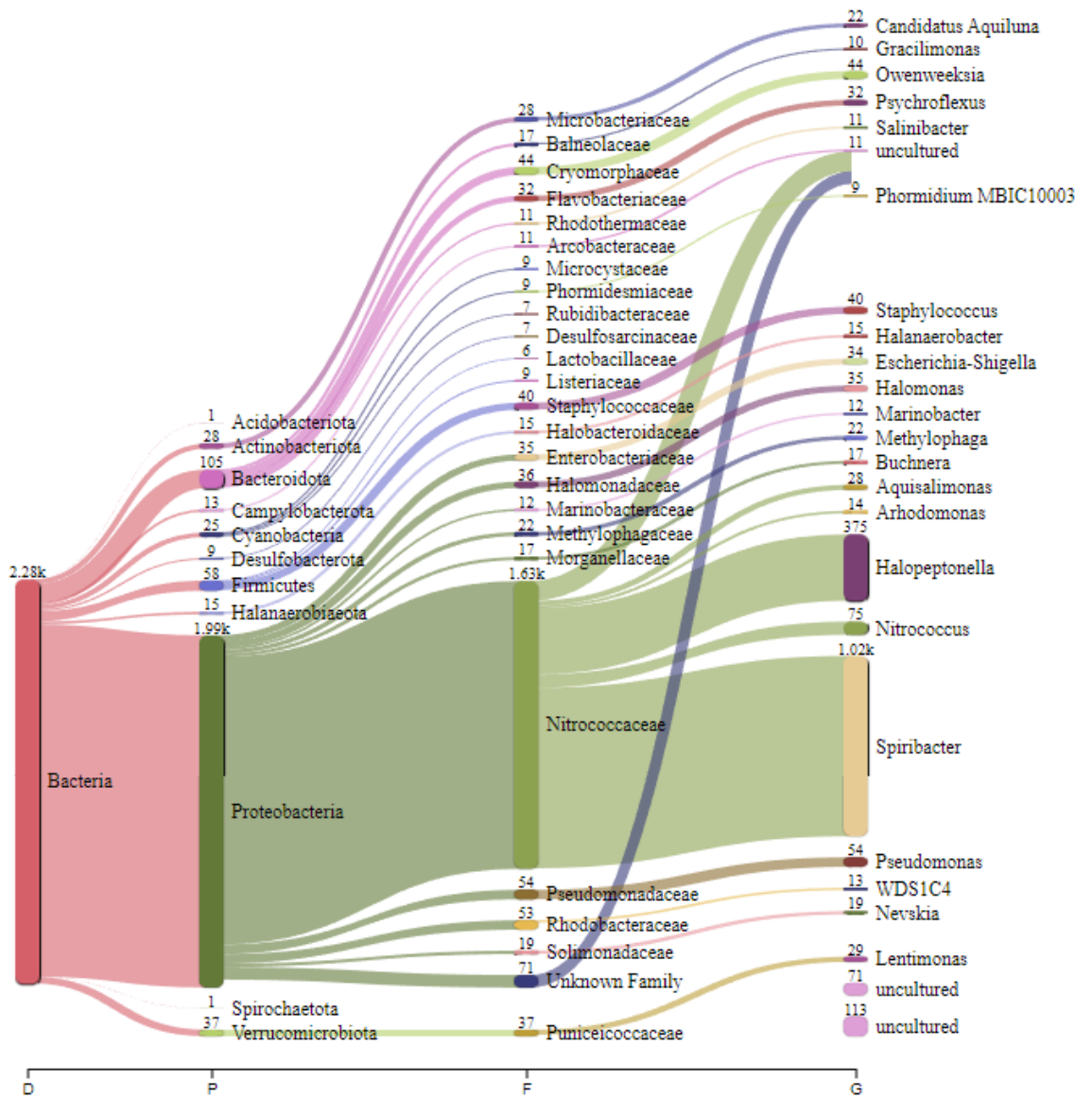
Figure S4. An example (WA1) of phylogenetic analysis of the most abundant genera in the West Aral Sea